

KRYLOV AND CORE TRANSFORMATION ALGORITHMS FOR AN INVERSE EIGENVALUE PROBLEM TO COMPUTE RECURRENCES OF MULTIPLE ORTHOGONAL POLYNOMIALS

AMIN FAGHIH, MICHELE RINELLI, MARC VAN BAREL, RAF VANDEBRIL,
AND ROBBE VERMEIREN

ABSTRACT. In this paper, we develop algorithms for computing the recurrence coefficients corresponding to multiple orthogonal polynomials on the step-line. We reformulate the problem as an inverse eigenvalue problem, which can be solved using numerical linear algebra techniques. We consider two approaches: the first is based on the link with block Krylov subspaces and results in a biorthogonal Lanczos process with multiple starting vectors; the second consists of applying a sequence of Gaussian eliminations on a diagonal matrix to construct the banded Hessenberg matrix containing the recurrence coefficients. We analyze the accuracy and stability of the algorithms with numerical experiments on the ill-conditioned inverse eigenvalue problems related to Kravchuk and Hahn polynomials, as well as on other better conditioned examples.

1. INTRODUCTION

Recently, there has been a renewed interest in multiple orthogonal polynomials (MOPs), which are an extension of the classical notion of orthogonal polynomials. This extension originates from simultaneous rational approximation, particularly from Hermite-Padé approximation, where multiple functions are approximated by rational functions with the same denominator [4, 6, 35]. MOPs are polynomials in one variable with orthogonality relations with respect to r measures $\mu_1, \mu_2, \dots, \mu_r$ [4, 6, 22, 30, 38]. In this text, we mainly deal with positive discrete measures on \mathbb{R} [7], which also arise in quadrature rules for continuous measures [37].

Let $\vec{n} = (n_1, n_2, \dots, n_r) \in \mathbb{N}^r$ be a multi-index with size $|\vec{n}| = n_1 + n_2 + \dots + n_r$. There exist two types of multiple orthogonal polynomials. Type I MOPs are tuples of polynomials $(A_{\vec{n},1}, \dots, A_{\vec{n},r})$, where $\deg A_{\vec{n},j} \leq n_j - 1$ for $j = 1, \dots, r$, that satisfy the orthogonality conditions

$$(1) \quad \int_{\mathbb{R}} \sum_{j=1}^r A_{\vec{n},j}(x) x^k d\mu_j(x) = 0, \quad 0 \leq k \leq |\vec{n}| - 2.$$

A type II multiple orthogonal polynomial $P_{\vec{n}}$ is a polynomial of degree at most $|\vec{n}|$ that satisfies

$$(2) \quad \int_{\mathbb{R}} P_{\vec{n}}(x) x^k d\mu_j = 0, \quad 0 \leq k \leq n_j - 1, \quad 1 \leq j \leq r.$$

Multiple orthogonal polynomials appear in various applications, such as rational approximation in number theory [4], evaluation of matrix functions [2], spectral theory of non-symmetric operators [3, 5], special function theory [6, 38], random matrix theory [23], eigenvalues of products of random matrices, non-intersecting Brownian motions, and combinatorial problems linked to random tilings [22, 23].

In 1969, Golub and Welsch [20] illustrated that in Gaussian quadrature (i.e., the case $r = 1$), the nodes and weights can be expressed in terms of eigenvalues and first components of the

eigenvectors of a Jacobi matrix, respectively. This Jacobi matrix contains the coefficients appearing in the three-term recurrence relation corresponding to the set of orthogonal polynomials. MOPs satisfy several recurrence relations depending on the path chosen for the multi-indices in \mathbb{N}^r . In this paper, we focus on the so-called step-line recurrence, an $(r+2)$ -term relation, resulting in a banded upper Hessenberg matrix¹ H_N taking the role of the Jacobi matrix [14, 22, 38]. As a consequence, the type I and type II MOPs are linked to the right and left eigenvectors of the recurrence matrix H_N , respectively; see, e.g., [12]. We propose numerical algorithms to compute these recurrence relations and recover the corresponding MOPs.

The Golub-Welsch approach was extended to multiple Gaussian quadrature by Borges [9], Coussement et al. [12], Van Assche [37], and Laudadio et al. [25], where the goal is to compute optimal nodes $\{z_i\}_{i=1}^N$ and weights $\{\alpha_{j,i}\}_{i=1}^N$ for $j = 1, 2, \dots, r$, to approximate integrals of a function f with respect to the different measures:

$$\int_{\mathbb{R}} f(x) d\mu_j(x) \approx \sum_{i=1}^N \alpha_{j,i} f(z_i).$$

We will be concerned with the opposite problem: given the nodes and weights of some discrete measures, we desire to retrieve the corresponding recurrence matrix. As explained in the previous paragraph, the nodes and weights are linked to the eigenvalues and eigenvectors of this recurrence matrix. Hence, we have an instance of an inverse eigenvalue problem (IEP) [8, 11].

We present two main algorithms for solving the IEP associated with MOPs. The first exploits the connection between MOPs and the pair of biorthogonal bases generated by a Lanczos-type algorithm with multiple starting vectors, which is a specialized version of the method described by Aliaga et al. [1]. The second is a core transformation algorithm which enforces the conditions specified in the IEP by iteratively executing Gaussian transformations on the diagonal matrix of nodes, generalizing the techniques developed by Mach, Van Barel, and Vandebril [27]. Both methods have been proven particularly effective in similar problems: generating orthogonal polynomials on the real line by solving an IEP associated with a Jacobi matrix [21, 33], constructing a set of biorthogonal polynomials following from the solution of a tridiagonal IEP [40], generating a sequence of (bi)orthogonal rational functions by solving a (tridiagonal) Hessenberg pencil IEP [43], and generating Sobolev orthogonal polynomials involving a Hessenberg IEP [41]. Furthermore, if one aims to do updating [43] and downdating [39], i.e. adding or removing a node in the discrete inner product, the core transformation approach is preferred. Finally, a third method exists, based on the Cholesky factorization of the moment matrix [40]. We briefly outline this approach, but do not study it in detail because of its less favorable numerical properties.

The computation of the step-line recurrence matrix H_N was already investigated by Filipuk, Haneczok and Van Assche [14], who proposed an algorithm to transform the recurrence coefficients of the individual measures into those for the multiple orthogonal polynomials (MOPs). Additionally, Milovanović and Stanić [29] introduced a discretized Stieltjes-Gautschi procedure for computing this recurrence matrix. This procedure expresses the entries of H_N in terms of the different inner products², which are then discretized using the corresponding Gaussian quadrature rules. Note that in our setting, this simplifies due to the assumption of discrete

¹In the literature, the recurrence relations are commonly written with a banded, lower Hessenberg matrix. However, we choose to work with the transpose of this matrix, as this matches more closely to the literature in numerical linear algebra, on which we will heavily rely.

²Every measure μ_j corresponds to an inner product $\langle f, g \rangle_{\mu_j} = \int_{\mathbb{R}} f(x)g(x)d\mu_j(x)$ of the functions f and g .

measures. Neither of these studies, however, explored the connection with Krylov subspaces or analyzed the numerical accuracy of the resulting methods. A systematic comparison of the performance of all these algorithms would be interesting for further research.

The paper is organized as follows: in section 2, the uniqueness conditions of type I and type II MOPs in a system of discrete measures are discussed. section 3 discusses the recurrence relations and formulates this as a matrix relation that leads to the formulation of the IEP. The link between Type I and block Krylov subspaces, and between Type II MOPs and standard Krylov subspaces, is explored in section 4. Also, we provide a Lanczos-type algorithm and discuss breakdown and reorthogonalization. In section 5, we describe the core transformation algorithm and illustrate its functioning with a small example. The outcome of both algorithms is the structured matrix whose elements are the recurrence coefficients for generating a sequence of biorthogonal type I and type II MOPs. In section 6, we test the correctness and accuracy of the proposed algorithms on the IEPs induced by the Kravchuk and Hahn MOPs, for which analytic formulae are derived in [7]. The poor performance is attributed to the ill-conditioning of the IEPs, as revealed by the Multiprecision toolbox Advanpix in MATLAB [32]; on the other hand, we get favorable results on artificial inner products with randomly generated weights, which turn out to be better conditioned. All MATLAB codes required to reproduce the experiments are publicly available³. Finally, section 7 gives a summary and discusses possible directions for future research.

2. UNIQUENESS OF TYPE I AND TYPE II MOPs

In this section, we analyze the existence and uniqueness of solutions to the linear systems (1) and (2) by introducing an algebraic Chebyshev system (AT system).

For the type II case, the usual requirement is that every possible solution of (2) has exactly degree $|\vec{n}|$. If this holds, we call \vec{n} a *normal index*. Since $P_{\vec{n}}$ is a polynomial of degree $|\vec{n}|$, equation (2) defines a homogeneous linear system of $|\vec{n}|$ equations with $|\vec{n}| + 1$ unknowns. The coefficient matrix $D^{(II)}$ of this system contains the moments of μ_j , i.e., $m_l^{(j)} = \int_{\mathbb{R}} x^l d\mu_j$. Let us define the block matrix $M_{\vec{n}}$ of size $|\vec{n}| \times |\vec{n}|$ as $M_{\vec{n}} = \begin{bmatrix} M_{n_1}^{(1)} & M_{n_2}^{(2)} & \dots & M_{n_r}^{(r)} \end{bmatrix}$, with the rectangular blocks

$$(3) \quad M_{n_j}^{(j)} = \begin{bmatrix} m_0^{(j)} & m_1^{(j)} & \dots & m_{n_j-1}^{(j)} \\ m_1^{(j)} & m_2^{(j)} & \dots & m_{n_j}^{(j)} \\ \vdots & \vdots & & \vdots \\ m_{|\vec{n}|-1}^{(j)} & m_{|\vec{n}|}^{(j)} & \dots & m_{|\vec{n}|+n_j-2}^{(j)} \end{bmatrix} \in \mathbb{R}^{|\vec{n}| \times n_j}.$$

Note that $M_{\vec{n}}^T$ is equal to the coefficient matrix $D^{(II)}$ with its last column removed. Hence, by checking that $M_{\vec{n}}^T$ is full rank, one can see if \vec{n} is a normal index.

A common requirement for a good definition of type I MOPs is that each $A_{\vec{n},j}$ has exactly degree $n_j - 1$. Note that the coefficient matrix of linear system (1) without its last column is equal to $M_{\vec{n}-\vec{1}}$. Thus, the above requirement is satisfied if $M_{\vec{n}-\vec{1}}$ has full rank.

To have a unique solution for systems (1) and (2), we need one additional requirement. For type II, we require the polynomials $P_{\vec{n}}$ to be monic. For type I, the following normalization

³<https://gitlab.kuleuven.be/numa/public/IEP-MOP>

condition is imposed

$$(4) \quad \int_{\mathbb{R}} \sum_{j=1}^r A_{\vec{n},j}(x) x^{|\vec{n}|-1} d\mu_j(x) = 1.$$

To find more details on the theory of MOPs, we refer the readers to the work of Coussemment and Van Assche [12], and Ismail [22].

In this paper, we restrict ourselves to discrete positive measures on \mathbb{R}

$$(5) \quad \mu_j = \sum_{i=1}^N \alpha_{j,i} \delta_{z_i}, \quad \alpha_{j,i} > 0, \quad z_i \in \mathbb{R}, \quad N \in \mathbb{N}, \quad 1 \leq j \leq r,$$

where all z_i are distinct, and δ_{z_i} denotes the Dirac measure at z_i . The support of these discrete measures is defined as $\text{supp}(\mu_j) = \{z_i\}_{i=1}^N$. Also denote $\Delta \subset \mathbb{R}$ as an interval that contains $\text{supp}(\mu_j)$ for all j .

2.1. AT system. An AT system is a particular set of measures such that every multi-index \vec{n} is normal. This subsection closely follows the discussion of Arvesú, Coussemment, and Van Assche [7].

Definition 2.1 (Chebyshev system). A linearly independent system of n basis functions $\alpha_1(x), \dots, \alpha_n(x)$ on $\Delta \subset \mathbb{R}$ is a Chebyshev system if every *non-trivial* linear combination $\sum_{k=1}^n a_k \alpha_k(x)$, with all $a_k \in \mathbb{R}$, has at most $n - 1$ zeros in Δ .

Definition 2.2 (AT system [7]). An AT system consists of r positive discrete measures $\{\mu_j\}_{j=1}^r$ (cf. (5)) with $\text{supp}(\mu_j) = \{z_i\}_{i=1}^N$ for all j , such that there exist r continuous functions $\alpha_j(x)$ on the interval Δ for which $\alpha_j(z_i) = \alpha_{j,i}$ for $j = 1, \dots, r$, $i = 1, \dots, N$ and the following $|\vec{n}|$ functions

$$\begin{aligned} & \alpha_1(x), x\alpha_1(x), \dots, x^{n_1-1}\alpha_1(x) \\ & \alpha_2(x), x\alpha_2(x), \dots, x^{n_2-1}\alpha_2(x) \\ & \vdots \\ & \alpha_r(x), x\alpha_r(x), \dots, x^{n_r-1}\alpha_r(x) \end{aligned}$$

give a Chebyshev system for each \vec{n} where $|\vec{n}| \leq N$.

The condition $|\vec{n}| \leq N$ is necessary for ensuring uniqueness. Indeed, suppose that $m = |\vec{n}| - N > 0$. Then we can take the polynomial $P_{\vec{n}}(x) = \prod_{i=1}^N (x - z_i) \prod_{i=1}^m (x - a_i)$ which will be a solution of system (2) for all a_1, \dots, a_m . It is important to note that if $|\vec{n}| = N$, then $P_{\vec{n}}(x) = (x - z_1)(x - z_2) \cdots (x - z_N)$.

The following theorem is a direct consequence of [7, Theorem 2.1], and ensures the uniqueness of MOPs in an AT system.

Theorem 2.3 (Uniqueness). *Assume we have an AT system with r positive discrete measures on Δ . Then for $|\vec{n}| \leq N$*

- *The coefficients of the type I polynomials $(A_{\vec{n},1}, \dots, A_{\vec{n},r})$, $\deg A_{\vec{n},j} = n_j - 1$, as the solution of the linear system (1) along with the normalization (4), can be uniquely determined.*
- *The linear system (2) has a unique set of coefficients defining the type II monic orthogonal polynomial $P_{\vec{n}}(x)$ of degree $|\vec{n}|$ as its solution.*

3. INVERSE EIGENVALUE PROBLEM

In this section, we discuss the connections between type I and type II MOPs, starting with their recurrence relations, followed by the biorthogonality property. Building upon these connections, we will subsequently formulate the problem of computing the recurrence coefficients as an inverse eigenvalue problem.

3.1. The step-line recurrence relation. Multiple orthogonal polynomials satisfy a number of recurrence relations depending on how the indices n_j are chosen. In this paper, we are concerned with the so-called step-line recurrence relation; see [22, Sec. 23.1.4] for a discussion on other recurrence relations. Let us define the monic type II MOPs on the step-line by

$$P_n(x) = P_{\vec{n}}(x), \quad \text{for } n = kr + \ell,$$

where r is the number of measures, and $\vec{n} = (\underbrace{k+1, \dots, k+1}_{\ell}, k, \dots, k)$.

It is known that the step-line monic polynomials $P_n(x)$ satisfy an $(r+2)$ -term recurrence relation; see e.g., [7, 12, 14, 22, 37, 38]

$$(6) \quad xP_n(x) = P_{n+1}(x) + \sum_{j=0}^r a_{n,j} P_{n-j}(x), \quad 0 \leq n \leq N-1,$$

with initial conditions $P_0 \equiv 1$ and $P_j \equiv 0$ for $j = -1, -2, \dots, -r$.

Let us define the discrete measure $\mu(x) = \sum_{i=1}^N \delta_{z_i}$, so that $d\mu_j(x) = \alpha_j(x)d\mu(x)$ ⁴ with $\alpha_j(z_i) = \alpha_{j,i}$ and zero elsewhere. We define the type I functions as

$$(7) \quad Q_{\vec{n}}(x) = \sum_{j=1}^r A_{\vec{n},j}(x) \alpha_j(x).$$

Note that, with this notation, the orthogonality relations (1) and the normalization condition (4) for type I MOPs become

$$(8) \quad \int_{\mathbb{R}} Q_{\vec{n}}(x) x^k d\mu(x) = \sum_{i=1}^N Q_{\vec{n}}(z_i) z_i^k = \begin{cases} 0, & 0 \leq k \leq |\vec{n}| - 2, \\ 1, & k = |\vec{n}| - 1. \end{cases}$$

The type I functions (7) fulfill a recurrence relation similar to (6), involving the same coefficients [22, 37]:

$$(9) \quad xQ_n(x) = Q_{n-1}(x) + \sum_{j=0}^r a_{n+j-1,j} Q_{n+j}(x), \quad 1 \leq n \leq N-r,$$

with initial conditions $Q_0 \equiv 0$ and Q_1, Q_2, \dots, Q_r .

For clarity and ease of implementation, we restrict ourselves to the case $r = 2$ for the remainder of the paper. For $sr = 2$, the type I functions (7) take the form

$$(10) \quad Q_n(x) = \alpha_1(x) A_{n,1}(x) + \alpha_2(x) A_{n,2}(x),$$

with $Q_n(x) := Q_{\vec{n}}(x)$, $A_{n,1}(x) := A_{\vec{n},1}(x)$ and $A_{n,2}(x) := A_{\vec{n},2}(x)$ where

$$(11) \quad \vec{n} = \begin{cases} (k, k), & n = 2k, \\ (k+1, k), & n = 2k+1. \end{cases}$$

⁴ μ_j is absolutely continuous with respect to μ .

In this setting, the step-line recurrence relation(6) becomes

$$(12) \quad xP_n(x) = P_{n+1}(x) + b_n P_n(x) + c_n P_{n-1}(x) + d_n P_{n-2}(x), \quad 0 \leq n \leq N-1,$$

while (9) is written as

$$(13) \quad xQ_n(x) = Q_{n-1}(x) + b_{n-1} Q_n(x) + c_n Q_{n+1}(x) + d_{n+1} Q_{n+2}(x), \quad 1 \leq n \leq N-r.$$

The coefficients of the recurrence relation (12) corresponding to $\{P_n(x)\}_{n=0}^{N-1}$ can be stored in a banded upper Hessenberg matrix

$$(14) \quad H_N = \begin{bmatrix} b_0 & c_1 & d_2 & 0 & 0 & 0 & \cdots & 0 \\ 1 & b_1 & c_2 & d_3 & 0 & 0 & \cdots & 0 \\ 0 & 1 & b_2 & c_3 & d_4 & 0 & \cdots & 0 \\ 0 & 0 & 1 & b_3 & c_4 & d_5 & \cdots & 0 \\ \vdots & & \ddots & \ddots & \ddots & \ddots & \ddots & \\ 0 & \cdots & 0 & 0 & 1 & b_{N-3} & c_{N-2} & d_{N-1} \\ 0 & \cdots & 0 & 0 & 0 & 1 & b_{N-2} & c_{N-1} \\ 0 & \cdots & 0 & 0 & 0 & 0 & 1 & b_{N-1} \end{bmatrix},$$

allowing us to write the step-line recurrence relation for the type II polynomials as

$$(15) \quad x[P_0(x) \dots P_{N-1}(x)] + [0 \dots P_N(x)] = [P_0(x) \dots P_{N-1}(x)] H_N.$$

Recall that $P_N(x)$ is the unique monic polynomial of degree N whose roots are the nodes $\{z_i\}_{i=1}^N$ associated with the measures μ_j , cf. (5). Thus, evaluating the above relation in z_i gives the following property.

Property 3.1. If $P_N(z_i) = 0$, then z_i is an eigenvalue of H_N corresponding to left eigenvector $v_{i,N} = [P_0(z_i) P_1(z_i) \dots P_{N-1}(z_i)]$.

By evaluating equations (15) in the nodes z_i , we obtain

$$(16) \quad ZV = VH_N,$$

with

$$(17) \quad V = \begin{bmatrix} P_0(z_1) & P_1(z_1) & \cdots & P_{N-1}(z_1) \\ P_0(z_2) & P_1(z_2) & \cdots & P_{N-1}(z_2) \\ \vdots & \vdots & & \vdots \\ P_0(z_N) & P_1(z_N) & \cdots & P_{N-1}(z_N) \end{bmatrix}, \quad Z = \begin{bmatrix} z_1 & & & \\ & z_2 & & \\ & & \ddots & \\ & & & z_N \end{bmatrix}.$$

Remark 3.2. The type I MOPs satisfy the same recurrence relation (13) of the type I functions (see, e.g., [22, Sec. 23.1.4]):

$$(18) \quad xA_{n,j}(x) = A_{n-1,j}(x) + b_{n-1}A_{n,j}(x) + c_nA_{n+1,j}(x) + d_{n+1}A_{n+2,j}(x),$$

for $n \geq 1$ and $j = 1, 2$. The fact that the measures form an AT-system implies that $d_{n+1} \neq 0$ for all $n = 1, \dots, N-2$. Indeed, if $n = 2k$ is even, we get from (11) that $\deg A_{n,2} = \deg A_{n+1,2} = k-1$ and $\deg A_{n+2,2} = k$. Hence, if we consider relation (18) for $j = 2$, the left-hand side is a polynomial of degree $k+1$, while the right-hand side has degree $k+1$ if and only if $d_{n+1} \neq 0$. If $n = 2k+1$ is odd, the same conclusion follows by observing that $\deg A_{n,1} = \deg A_{n+1,1} = k$ and $\deg A_{n+2,1} = k+1$.

3.2. The inverse eigenvalue problem. In this section, we formalize the problem of generating MOPs associated with a discrete inner product as an inverse eigenvalue problem. Before doing this, we require one additional result establishing a biorthogonality relation between the type I functions and the type II monic polynomials. Given the discrete positive measures μ_j as in equation (5), we define a discrete inner product for type I functions and type II monic polynomials on the step line, with real, positive weights $\{\alpha_{j,i}\}_{i=1}^N$, $j = 1, 2$, and distinct nodes $\{z_i\}_{i=1}^N$, $z_i \in \mathbb{R}$, as

$$(19) \quad \langle P_n, Q_m \rangle_N = \sum_{i=1}^N P_n(z_i) Q_m(z_i) = \sum_{i=1}^N P_n(z_i) (\alpha_{1,i} A_{m,1}(z_i) + \alpha_{2,i} A_{m,2}(z_i)).$$

Proposition 3.3 (Chapter 23 of [22]). *Given the type I functions as defined in (10) and the type II monic polynomials on the step-line, the following biorthogonality with respect to $\langle \cdot, \cdot \rangle_N$ holds:*

$$(20) \quad \langle P_n, Q_m \rangle_N = \begin{cases} 0, & m \leq n, \\ 0, & n \leq m - 2, \\ 1, & m = n + 1. \end{cases}$$

This result follows directly from the orthogonality conditions of type I and type II polynomials. The case where $m = n + 1$ holds because of the additional normalization relation for type I (4). In order to reformulate Proposition 3.3, we construct a matrix W of size $N \times N$ as

$$W = \begin{bmatrix} Q_1(z_1) & Q_2(z_1) & \cdots & Q_N(z_1) \\ Q_1(z_2) & Q_2(z_2) & \cdots & Q_N(z_2) \\ \vdots & \vdots & & \vdots \\ Q_1(z_N) & Q_2(z_N) & \cdots & Q_N(z_N) \end{bmatrix}.$$

Relation 20 now becomes

$$(21) \quad W^T V = I_N,$$

with I_N the identity matrix of size $N \times N$. By combining the biorthogonality relation (21) with equation (16), the identities $ZW = WH_N^T$ and $H_N = W^T ZV$ are both equivalent to relation (16). Moreover, the i th-row of W is a right eigenvector of H_N corresponding to the eigenvalue z_i . The first and the second components of these right eigenvectors can be retrieved using the following result from Van Assche⁵ [37, Theorem 2].

Theorem 3.4. *Given nodes $\{z_i\}_{i=1}^N$, and weight vectors $\alpha_1 = [\alpha_{1,1} \dots \alpha_{1,N}]^T$ and $\alpha_2 = [\alpha_{2,1} \dots \alpha_{2,N}]^T$ from the discrete measures μ_1 and μ_2 in equation (5), one can compute the first and second column of W as*

$$\begin{aligned} \alpha_1 &= d_1 w_1, \\ \alpha_2 &= d_2 w_1 + d_3 w_2, \end{aligned}$$

⁵Van Assche used this result in the context of Gaussian quadrature. He assumed that the first and second components of the right eigenvectors were given and calculated the optimal quadrature weights $\alpha_{1,j}$, $\alpha_{2,j}$.

where d_1 , d_2 , and d_3 are constants given by

$$\begin{aligned} d_1 &= \int_{\mathbb{R}} P_0(x) d\mu_1(x) = \sum_{i=1}^N \alpha_{1,i} P_0(z_i), & d_2 &= \int_{\mathbb{R}} P_0(x) d\mu_2(x) = \sum_{i=1}^N \alpha_{2,i} P_0(z_i), \\ d_3 &= \int_{\mathbb{R}} P_1(x) d\mu_2(x) = \sum_{i=1}^N \alpha_{2,i} P_1(z_i). \end{aligned}$$

We can now state the main problem formally. We start with the general formulation.

Problem 3.5 (Generating MOPs). Let a discrete inner product $\langle \cdot, \cdot \rangle_N$ as in 19 be given, with nodes $\{z_i\}_{i=1}^N$ and a pair of weights $\{\alpha_{1,i}\}_{i=1}^N$, and $\{\alpha_{2,i}\}_{i=1}^N$. Compute a sequence of biorthogonal type I functions $\{Q_n\}_{n=1}^N = \{\alpha_1 A_{n,1} + \alpha_2 A_{n,2}\}_{n=1}^N$ and type II monic polynomials $\{P_n\}_{n=0}^{N-1}$ at the given nodes z_i satisfying 20.

Problem 3.5 can be reformulated as an inverse eigenvalue problem. Here and throughout the rest of this paper, we denote the recurrence matrix by H when the dependence of the size is clear from the context.

Problem 3.6. Given a diagonal matrix $Z = \text{diag}(\{z_i\}_{i=1}^N) \in \mathbb{R}^{N \times N}$ with distinct nodes, and vectors $\mathbf{w}_1, \mathbf{w}_2, \mathbf{v}_1 \in \mathbb{R}^N$ satisfying

$$(22) \quad \mathbf{w}_1^T \mathbf{v}_1 = 1, \quad \mathbf{w}_2^T \mathbf{v}_1 = 0, \quad \text{and} \quad \mathbf{w}_2^T Z \mathbf{v}_1 = 1,$$

construct a Hessenberg matrix $H \in \mathbb{R}^{N \times N}$, as in (14), and a pair of matrices $W, V \in \mathbb{R}^{N \times N}$ such that

(D1) The first two columns of W equal \mathbf{w}_1 and \mathbf{w}_2 and the first column of V is \mathbf{v}_1 :

$$\begin{bmatrix} | & | \\ \mathbf{w}_1 & \mathbf{w}_2 \\ | & | \end{bmatrix} = W \begin{bmatrix} | & | \\ \mathbf{e}_1 & \mathbf{e}_2 \\ | & | \end{bmatrix}, \quad \text{and} \quad \begin{bmatrix} | \\ \mathbf{v}_1 \\ | \end{bmatrix} = V \begin{bmatrix} | \\ \mathbf{e}_1 \\ | \end{bmatrix},$$

(D2) $W^T V = I_N$ (biorthogonality),

(D3) $W^T Z V = H$.

Solving this IEP is equivalent to computing a sequence of biorthogonal type I functions and type II MOPs, orthogonal with respect to the discrete inner product 19. We obtain the vectors $\mathbf{w}_1, \mathbf{w}_2, \mathbf{v}_1$ by using the following proposition, which is a direct application of Theorem 3.4.

Proposition 3.7. Assume we have an AT system (2.2) with the positive discrete measures μ_1 and μ_2 as in (5). Then, the starting vectors $\mathbf{w}_1, \mathbf{w}_2$ and \mathbf{v}_1 for Problem 3.6 are given as

$$\begin{aligned} \mathbf{w}_1 &= \frac{1}{d_1} \boldsymbol{\alpha}_1, & \mathbf{v}_1 &= [1 \quad 1 \quad \dots \quad 1]^T, \\ \mathbf{w}_2 &= \frac{1}{d_3} (\boldsymbol{\alpha}_2 - d_2 \mathbf{w}_1), \end{aligned}$$

where

$$d_1 = \sum_{i=1}^N \alpha_{1,i}, \quad d_2 = \sum_{i=1}^N \alpha_{2,i}, \quad d_3 = \sum_{i=1}^N \left(z_i - \frac{\sum_{j=1}^N z_j \alpha_{1,j}}{\sum_{j=1}^N \alpha_{1,j}} \right) \alpha_{2,i}.$$

Proof. It follows from Problem 3.6 that $\mathbf{v}_1 = [P_0(z_0) \ P_0(z_1) \ \cdots \ P_0(z_N)]^T$. From the definition of type II MOPs, P_0 is a monic polynomial of degree 0 and thus $P_0 = 1$. Applying Theorem 3.4, we directly obtain the expressions for \mathbf{w}_1 and \mathbf{w}_2 . Likewise, the formulas for d_1 and d_2 follow immediately. To compute d_3 , one needs the monic type II polynomial $P_1(x) = x + c$. The constant c can be determined by imposing the orthogonality of P_1 with respect to the measure μ_1

$$\int_{\mathbb{R}} P_1(x) d\mu_1(x) = \sum_{j=1}^N (z_j + c) \alpha_{1,j} = 0,$$

which gives

$$c = \frac{-\sum_{j=1}^N z_j \alpha_{1,j}}{\sum_{j=1}^N \alpha_{1,j}}.$$

Now, d_3 can be computed as

$$d_3 = \int_{\mathbb{R}} P_1(x) d\mu_2(x) = \sum_{i=1}^N (z_i + c) \alpha_{2,i}.$$

□

As already mentioned, the focus is on $r = 2$, although everything can be extended to a general $r \geq 2$. For general r , the banded recurrence matrix H will have r superdiagonals. Coussement and Van Assche [12, Theorem 3.2] proved the extension of Theorem 3.4 for general r which can be used to find the initial vectors $\mathbf{w}_1, \mathbf{w}_2, \dots, \mathbf{w}_r$ to solve the corresponding inverse eigenvalue problem.

4. CONNECTION WITH (BLOCK) KRYLOV SUBSPACES

In this section, we discuss the connection between Krylov subspaces and MOPs. By exploiting this relationship, we specialize the Lanczos-like procedure with multiple starting vectors, as developed by Aliaga et al. [1], to solve Problem 3.6. Given a matrix $M \in \mathbb{R}^{N \times N}$ and a starting vector $\mathbf{v}_1 \in \mathbb{R}^{N \times N}$, we define the Krylov subspace

$$(23) \quad \mathcal{K}_m(M, \mathbf{v}_1) = \text{span}\{\mathbf{v}_1, M\mathbf{v}_1, \dots, M^{m-1}\mathbf{v}_1\}.$$

Krylov methods are based on the projection of the matrix M onto $\mathcal{K}_m(M, \mathbf{v}_1)$. Since the spanning vectors in (23) are usually close to being linearly dependent, one typically computes a different basis. An orthonormal basis $V_m = [\mathbf{v}_1, \mathbf{v}_2, \dots, \mathbf{v}_m]$ of $\mathcal{K}_m(M, \mathbf{v}_1)$ (here we assume that $\|\mathbf{v}_1\| = 1$) can be computed sequentially by the Arnoldi algorithm, which reduces to the three-term recurrence of Lanczos if M is symmetric. The basis is also nested, meaning that $\{\mathbf{v}_1, \dots, \mathbf{v}_i\}$ is a basis of $\mathcal{K}_i(M, \mathbf{v}_1)$ for all $i \leq m$. Other approaches include biorthogonal methods, for which the projection onto $\mathcal{K}_m(M, \mathbf{v}_1)$ is orthogonal to another Krylov subspace $\mathcal{K}_m(M^T, \mathbf{w}_1)$ where $\mathbf{w}_1^T \mathbf{v}_1 = 1$. For instance, the biorthogonal Lanczos algorithm (see, e.g., [34, Algorithm 7.1]) generates matrices $V_m, W_m \in \mathbb{R}^{N \times m}$, whose columns form bases of $\mathcal{K}_m(M, \mathbf{v}_1)$ and $\mathcal{K}_m(M^T, \mathbf{w}_1)$, respectively, and satisfy the biorthogonality condition $W_m^T V_m = I_m$. The columns of V_m and W_m satisfy three-term recurrence relations, and the projection $W_m^T M V_m$ is tridiagonal.

When considering multiple starting vectors, one can use block variants of Krylov subspaces. Given two starting vectors $\mathbf{w}_1, \mathbf{w}_2 \in \mathbb{R}^N$ (for the general case see, e.g., [1, 16]), we define the

block Krylov subspace as

$$(24) \quad \mathcal{K}_m^\square(M, [\mathbf{w}_1, \mathbf{w}_2]) = \begin{cases} \mathcal{K}_k(M, \mathbf{w}_1) + \mathcal{K}_k(M, \mathbf{w}_2) & \text{if } m = 2k, \\ \mathcal{K}_{k+1}(M, \mathbf{w}_1) + \mathcal{K}_k(M, \mathbf{w}_2) & \text{if } m = 2k + 1. \end{cases}$$

For notational convenience, the elements of $\mathcal{K}_m^\square(M, [\mathbf{w}_1, \mathbf{w}_2])$ are vectors. In other common notations, the block Krylov subspace consists of block vectors; see, e.g., [26]. However, the latter notation makes it harder to deal with odd indices, as it's needed Classical Krylov methods, such as the Arnoldi and Lanczos algorithms, can be extended to the block setting [16]. Aliaga et al. [1] study a biorthogonal Lanczos-type algorithm for computing a pair of biorthogonal bases of two block Krylov subspaces with a possibly different number of starting vectors, and the recurrence matrix is banded, with the lower and upper bandwidths depending on the number of starting vectors of each subspace. Algorithm 1 gives a specialized version for solving Problem 3.6.

Krylov subspaces are profoundly linked with polynomials. For the standard case, every element $\mathbf{v} \in \mathcal{K}_m(M, \mathbf{v})$ can be expressed as $\mathbf{v} = p_{m-1}(M)\mathbf{v}_1$, where p_{m-1} is a polynomial of degree at most $m - 1$. Moreover, the orthonormal basis generated by the Arnoldi algorithm corresponds to a system of orthogonal polynomials associated with a suitable inner product; see, e.g., [18]. On the other hand, for $\mathbf{w} \in \mathcal{K}_m^\square(M, [\mathbf{w}_1, \mathbf{w}_2])$, it follows from equation (24) that $\mathbf{w} = p(A)\mathbf{w}_1 + q(A)\mathbf{w}_2$, where p and q are polynomials of appropriate degree.

Alqahtani and Reichel [2] show that, for a symmetric M , the Krylov subspaces $\mathcal{K}_m(M, \mathbf{v}_1)$, $\mathcal{K}_m^\square(M^T, [\mathbf{w}_1, \mathbf{w}_2])$ are linked to an unweighted, indefinite inner product and the associated MOPs of type II and I, respectively. Here, we do the opposite: given a family of inner products and the associated MOPs, we link them with the appropriate Krylov subspaces and biorthogonal bases.

The link between inverse eigenvalue problems and Krylov subspace methods is not new in the literature. For example, the Lanczos or Arnoldi algorithms can be used to solve an IEP with orthonormal eigenvectors and tridiagonal or Hessenberg structure [8], while rational Krylov methods can be used for IEPs with a pencil formulation [42, 43]. The following result shows the connection between the IEP in Problem 3.6 and Krylov subspaces.

Proposition 4.1. *Let $Z = \text{diag}(z_1, \dots, z_N)$, $\mathbf{w}_1, \mathbf{w}_2$ and \mathbf{v}_1 be as in Problem 3.6. Suppose that the IEP admits a solution, i.e., $V = [\mathbf{v}_1, \dots, \mathbf{v}_N]$, $W = [\mathbf{w}_1, \dots, \mathbf{w}_N]$, and H with the structure (14) such that $W^T Z V = H$ and $W^T V = I_N$. Furthermore, assume that $d_n \neq 0$ (cf. Remark 3.2) for $n = 2, \dots, N - 1$. Then, for $m \leq N$, the sets $\{\mathbf{v}_i\}_{i=1}^m$ and $\{\mathbf{w}_i\}_{i=1}^m$ form a basis of $\mathcal{K}_m(Z, \mathbf{v}_1)$ and $\mathcal{K}_m^\square(Z, [\mathbf{w}_1, \mathbf{w}_2])$, respectively.*

Proof. Since $W^T V = I_N$, the matrices V and W are both invertible. Hence, both the sets $\{\mathbf{v}_1, \dots, \mathbf{v}_m\}$ and $\{\mathbf{w}_1, \dots, \mathbf{w}_m\}$ form a system of linearly independent vectors. To prove both statements, it suffices to show that $\mathbf{v}_n \in \mathcal{K}_n(Z, \mathbf{v}_1)$ and $\mathbf{w}_n \in \mathcal{K}_n^\square(Z, [\mathbf{w}_1, \mathbf{w}_2])$ for all $n = 1, \dots, N$, since then $\{\mathbf{v}_1, \dots, \mathbf{v}_m\} \subset \mathcal{K}_m(Z, \mathbf{v}_1)$ and $\{\mathbf{w}_1, \dots, \mathbf{w}_m\} \subset \mathcal{K}_m^\square(Z, [\mathbf{w}_1, \mathbf{w}_2])$, and we conclude using the fact that the dimension of both subspaces is at most m .

1. Let us show that $\mathbf{v}_n \in \mathcal{K}_n(Z, \mathbf{v}_1)$ by induction. By definition, we have that $\mathbf{v}_1 \in \mathcal{K}_1(Z, \mathbf{v}_1)$. From the relation $ZV = VH$ and the structure of H in equation (14), we get that

$$(25) \quad \mathbf{v}_{n+1} = Z\mathbf{v}_n - b_n\mathbf{v}_n - c_n\mathbf{v}_{n-1} - d_n\mathbf{v}_{n-2} \quad \text{for } n = 1, \dots, N - 1,$$

where we assume $\mathbf{v}_{-1}, \mathbf{v}_0 = 0$ and $c_0, d_0, d_1 = 0$. Hence, since $\mathbf{v}_n, \mathbf{v}_{n-1}, \mathbf{v}_{n-2} \in \mathcal{K}_n(Z, \mathbf{v}_1)$ by inductive hypothesis, and $Z\mathbf{v}_n \in Z\mathcal{K}_n(Z, \mathbf{v}_1) \subset \mathcal{K}_{n+1}(Z, \mathbf{v}_1)$, we have that

$$\mathbf{v}_{n+1} \in \text{span}\{Z\mathbf{v}_n, \mathbf{v}_n, \mathbf{v}_{n-1}, \mathbf{v}_{n-2}\} \subset \mathcal{K}_{n+1}(Z, \mathbf{v}_1),$$

for all $n = 1, \dots, N - 1$.

2. Now we show that $\mathbf{w}_n \in \mathcal{K}_n^\square(Z, [\mathbf{w}_1, \mathbf{w}_2])$. By definition, we have that $\mathbf{w}_1 \in \mathcal{K}_1^\square(Z, [\mathbf{w}_1, \mathbf{w}_2])$ and $\mathbf{w}_2 \in \mathcal{K}_2^\square(Z, [\mathbf{w}_1, \mathbf{w}_2])$. In this case, we use the relation $ZW = WH^T$ and get that for $n = 1, \dots, N - 1$,

$$(26) \quad \mathbf{w}_{n+1} = \frac{1}{d_n} (Z\mathbf{w}_{n-1} - c_{n-1}\mathbf{w}_n - b_{n-2}\mathbf{w}_{n-1} - \mathbf{w}_{n-2}).$$

By inductive hypothesis, we have that $\mathbf{w}_n, \mathbf{w}_{n-1}, \mathbf{w}_{n-2} \in \mathcal{K}_n^\square(Z, [\mathbf{w}_1, \mathbf{w}_2])$. Therefore, from the definition of the block Krylov subspace, we get that $Z\mathbf{w}_{n-1} \in Z\mathcal{K}_{n-1}^\square(Z, [\mathbf{w}_1, \mathbf{w}_2]) \subset \mathcal{K}_{n+1}^\square(Z, [\mathbf{w}_1, \mathbf{w}_2])$. Finally,

$$\mathbf{w}_{n+1} \in \text{span}\{Z\mathbf{w}_{n-1}, \mathbf{w}_n, \mathbf{w}_{n-1}, \mathbf{w}_{n-2}\} \subset \mathcal{K}_{n+1}^\square(Z, [\mathbf{w}_1, \mathbf{w}_2]),$$

which concludes the proof. \square

4.1. A biorthogonal Lanczos algorithm. By Proposition 4.1, a solution of Problem 3.6 consists of a recurrence matrix H and a pair V and W of biorthogonal bases which are nested for the corresponding Krylov subspaces. We consider Algorithm 1 for solving Problem 3.6.

Algorithm 1 IEP_KRYL

Require: Diagonal matrix $Z = \text{diag}(z_1, \dots, z_N)$, vectors $\mathbf{w}_1, \mathbf{w}_2, \mathbf{v}_1 \in \mathbb{R}^n$ such that $\mathbf{w}_1^T \mathbf{v}_1 = 1$, $\mathbf{w}_2^T \mathbf{v}_1 = 0$, $\mathbf{w}_2^T Z\mathbf{v}_1 = 1$.

Ensure: $W = [\mathbf{w}_1, \dots, \mathbf{w}_N]$, $V = [\mathbf{v}_1, \dots, \mathbf{v}_N] \in \mathbb{R}^{N \times N}$ such that $W^T V = I_N$, and entries b_0, \dots, b_{N-1} , c_1, \dots, c_{N-1} , d_2, \dots, d_{N-1} of the banded Hessenberg matrix H as in equation (14) such that $W^T ZV = H$

- 1: $b_0 = \mathbf{w}_1^T Z\mathbf{v}_1$
 - 2: $\mathbf{v}_2 = Z\mathbf{v}_1 - b_0\mathbf{v}_1$
 - 3: $b_1 = \mathbf{w}_2^T Z\mathbf{v}_2$, $c_1 = \mathbf{w}_1^T Z\mathbf{v}_2$
 - 4: $\mathbf{v}_3 = Z\mathbf{v}_2 - b_1\mathbf{v}_2 - c_1\mathbf{v}_1$
 - 5: $\hat{\mathbf{w}}_3 = Z\mathbf{w}_1 - c_1\mathbf{w}_2 - b_0\mathbf{w}_1$
 - 6: $d_2 = \mathbf{w}_1^T Z\mathbf{v}_3$, $\mathbf{w}_3 = \hat{\mathbf{w}}_3/d_2$
 - 7: **for** $n = 3 : N - 1$ **do**
 - 8: $b_{n-1} = \mathbf{w}_n^T Z\mathbf{v}_n$, $c_{n-1} = \mathbf{w}_{n-1}^T Z\mathbf{v}_n$
 - 9: $\mathbf{v}_{n+1} = Z\mathbf{v}_n - b_{n-1}\mathbf{v}_n - c_{n-1}\mathbf{v}_{n-1} - d_{n-1}\mathbf{v}_{n-2}$
 - 10: $\hat{\mathbf{w}}_{n+1} = Z\mathbf{w}_{n-1} - c_{n-1}\mathbf{w}_n - b_{n-2}\mathbf{w}_{n-1} - \mathbf{w}_{n-2}$
 - 11: $d_n = \mathbf{w}_{n-1}^T Z\mathbf{v}_{n+1}$
 - 12: $\mathbf{w}_{n+1} = \hat{\mathbf{w}}_{n+1}/d_n$
 - 13: **end for**
 - 14: $b_{N-1} = \mathbf{w}_N^T Z\mathbf{v}_N$, $c_{N-1} = \mathbf{w}_{N-1}^T Z\mathbf{v}_N$
-

By construction, the outputs satisfy the recurrence relations $ZV = VH$, $ZW = WH^T$, along with the biorthogonality conditions $\mathbf{w}_{n+1}^T \mathbf{v}_k = \mathbf{w}_k^T \mathbf{v}_{n+1} = 0$, for each n and $k = n - 2, n - 1, n$. To show this for all n and k , thus obtaining $W^T V = I_N$, one can use an induction argument, as done in [34, Proposition 7.1] for the classical biorthogonal Lanczos algorithm. Moreover, H has the structure described in (14). Since $\mathbf{w}_{n-2}, \mathbf{w}_{n-1}, \mathbf{w}_n$ are all orthogonal to \mathbf{v}_{n+1} , Line 11 can be replaced by the assignment $d_n = \mathbf{w}_{n+1}^T \mathbf{v}_{n+1}$, which is more common in the literature [34]. Algorithm 1 consists of a few vector sums, Euclidean inner products and

scalar multiplications per iteration, for which the cost is $O(N)$. Thus, the overall complexity is $\mathcal{O}(N^2)$.

If the algorithm successfully terminates, we are able to prove the uniqueness of the solution for Problem 3.6.

Proposition 4.2. *If no breakdown occurs in Algorithm 1, then Problem 3.6 admits a unique solution.*

Proof. Let V, W, H be any solution of Problem 3.6, and denote by $\mathbf{v}_1, \dots, \mathbf{v}_N, \mathbf{w}_1, \dots, \mathbf{w}_N$ the columns of V and W , respectively, and by $b_0, \dots, b_{N-1}, c_1, \dots, c_{N-1}, d_2, \dots, d_{N-1}$ the entries of H as in equation (14). Since $H = W^T ZV$ and $[H]_{i,j} = \mathbf{w}_i^T Z\mathbf{v}_j$, we get that

$$(27) \quad b_{n-1} = \mathbf{w}_n^T Z\mathbf{v}_n, \quad c_{n-1} = \mathbf{w}_{n-1}^T Z\mathbf{v}_n, \quad d_n = \mathbf{w}_{n-1}^T Z\mathbf{v}_{n+1}.$$

Moreover, because of the identities $ZV = VH$ and $ZW = WH^T$, the basis vectors in the columns of V and W satisfy the recurrence relations (25) and (26), respectively, assuming that $\mathbf{v}_{-1}, \mathbf{v}_0, \mathbf{w}_{-1}, \mathbf{w}_0 = 0$ and $c_0, d_0, d_1 = 0$. Hence, by induction, it follows that the solution coincides with the outcome of Algorithm 1. \square

4.2. Numerical aspects. Biorthogonal Krylov methods often suffer from numerical issues. Here, we discuss how they affect the solution of Problem 3.6 via Algorithm 1 and possible strategies to overcome them.

A breakdown occurs in Line 11 if d_n equals zero. Remark 3.2 ensures that this cannot happen when the IEP is associated with some classes of well-defined MOPs. However, this does not exclude the possibility of a near-breakdown, which arises when d_n is small. A popular workaround for this issue is the look-ahead technique which is described, for instance, by Freund [15] for the standard biorthogonal Lanczos method and extended by Aliaga et al. [1] to the case of multiple starting vectors. However, this approach changes the sparsity pattern of the recurrence matrix by introducing nonzero entries outside the prescribed bandwidth, thereby perturbing the required structure in Problem 3.6. We also found that the near-breakdown, unlike other phenomena, is not the main source of inaccuracy in our tests as we will explain in section 6. Although we implemented look-ahead techniques in our algorithms, they did not lead to improved accuracy. Therefore, we omit them from both the discussion and the final algorithmic formulations.

A feature of Algorithm 1 is that it returns H with lower subdiagonal entries equal to 1. This is because \mathbf{v}_{n+1} is not scaled after its orthogonalization at Line 9, while the scaling is concentrated on \mathbf{w}_{n+1} at Line 12, as required in Problem 3.6. These ones on the subdiagonal correspond to the choice of monic type II MOPs as discussed in section 3.1. Numerically, the resulting pair of bases are typically severely ill-conditioned, implying that neither the biorthogonality condition $W^T V = I_N$ nor $W^T ZV = H$ will be satisfied in practice. Different scaling strategies can be used to mitigate this high conditioning number. For example, by imposing that all basis vectors have unit norm, the biorthogonality relation reduces to $W^T V = \Sigma$, where Σ is a diagonal matrix, though not necessarily the identity. As a consequence, V and W will satisfy the two recurrence relations

$$ZV = VH_V, \quad ZW = WH_W,$$

where $(H_W)^T$ and H_V have the same sparsity pattern as in equation (14) but without the ones on the subdiagonal. We can get biorthonormal bases through a diagonal scaling. More specifically, if $W^T V = \Sigma_1 \Sigma_2$, for any diagonal matrices Σ_1 and Σ_2 , then $\widetilde{W} = W\Sigma_1^{-1}$ and $\widetilde{V} = V\Sigma_2^{-1}$ satisfy $\widetilde{W}^T \widetilde{V} = I_N$. Furthermore, we get that $\Sigma_1 H_V \Sigma_1^{-1} = \Sigma_2^{-1} (H_W)^T \Sigma_2 =: H$

satisfies $\widetilde{W}^T Z \widetilde{V} = H$. The ones on the subdiagonal may be obtained via an additional diagonal scaling as is described for $N = 5$ in equation (30); for the general case, see [24, Sec. 6]. As previously mentioned, the solutions W and V corresponding to monic type II MOPs are ill-conditioned, so performing the appropriate scaling is not feasible in practice.

The orthogonalization process in Algorithm 1 relies on the short recurrences at lines 9 and 10. In order to get \mathbf{v}_{n+1} and \mathbf{w}_{n+1} , we only need to orthogonalize $Z\mathbf{v}_n$ and $Z\mathbf{w}_{n-1}$ against $\mathbf{w}_{n-2}, \mathbf{w}_{n-1}, \mathbf{w}_n$ and $\mathbf{v}_{n-2}, \mathbf{v}_{n-1}, \mathbf{v}_n$, respectively. In fact, in exact arithmetic, $Z\mathbf{v}_n$ is orthogonal to $\mathcal{K}_{n-3}^\square(Z, [\mathbf{w}_1, \mathbf{w}_2])$ and $Z\mathbf{w}_{n-1}$ is orthogonal to $\mathcal{K}_{n-3}(Z, \mathbf{v}_1)$. However, numerically, the quantities $\mathbf{w}_i^T \mathbf{v}_{n+1}$ and $\mathbf{w}_{n+1}^T \mathbf{v}_j$ may not be small. This phenomenon affects most Krylov subspace methods and is referred to as loss of orthogonality. To address this issue, one could perform a full biorthogonalization instead of relying on the short recurrence relation. To further ensure the biorthogonality, we can also apply reorthogonalization to the computed bases W and V , at the cost of another long-term recurrence formula for each step. For further details and strategies like selective reorthogonalization, see [31].

In algorithm 2 we consider a process including the aforementioned techniques. According to the MATLAB notation, we denote by $H(i, j)$ the (i, j) entry of H , and by $H(i_1 : i_2, j_1 : j_2)$ the submatrix of H with indices (i, j) , $i_1 \leq i \leq i_2$, $j_1 \leq j \leq j_2$.

Algorithm 2 IEP_KRYLREORTH

Require: Diagonal matrix $Z = \text{diag}(z_1, \dots, z_N)$, vectors $\mathbf{w}_1, \mathbf{w}_2, \mathbf{v}_1 \in \mathbb{R}^n$ such that $\mathbf{w}_1^T \mathbf{v}_1 = 1$, $\mathbf{w}_2^T \mathbf{v}_1 = 0$, $\mathbf{w}_2^T Z \mathbf{v}_1 \neq 1$, and $\|\mathbf{v}_1\| = \|\mathbf{w}_1\| = \|\mathbf{w}_2\| = 1$, orthogonalization strategy **partial** or **full**

Ensure: $W = [\mathbf{w}_1, \dots, \mathbf{w}_N]$, $V = [\mathbf{v}_1, \dots, \mathbf{v}_N]$, and $\Sigma = \text{diag}(\sigma_1, \dots, \sigma_N)$ such that $W^T V = \Sigma$ and $\|\mathbf{v}_n\| = \|\mathbf{w}_n\| = 1$ for all n , and recurrence matrices H_V, H_W such that $ZV = V H_V$ and $ZW = W H_W$.

- 1: $\sigma_1 = \mathbf{w}_1^T \mathbf{v}_1$, $H_V(1, 1) = \mathbf{w}_1^T Z \mathbf{v}_1 / \sigma_1$
 - 2: $\hat{\mathbf{v}}_2 = Z \mathbf{v}_1 - H_V(1, 1) \mathbf{v}_1$
 - 3: $H_V(2, 1) = \|\hat{\mathbf{v}}_2\|$, $\mathbf{v}_2 = \hat{\mathbf{v}}_2 / H_V(2, 1)$, $\sigma_2 = \mathbf{w}_2^T \mathbf{v}_2$
 - 4: **for** $n = 2 : N - 1$ **do**
 - 5: $\hat{\mathbf{v}}_{n+1} = Z \mathbf{v}_n$, $\hat{\mathbf{w}}_{n+1} = Z \mathbf{w}_{n-1}$
 - 6: Orthogonalization: set $r = \max(1, n - 2)$ for **partial**, $r = 1$ for **full**
 - 7: Set $V_n = [\mathbf{v}_r, \dots, \mathbf{v}_n]$, $W_n = [\mathbf{w}_r, \dots, \mathbf{w}_n]$, and $\Sigma_n = \text{diag}(\sigma_r, \dots, \sigma_n)$
 - 8: $H_V(r : n, n) = \Sigma_n^{-1} W_n^T \hat{\mathbf{v}}_{n+1}$, $H_W(r : n, n - 1) = \Sigma_n^{-1} V_n^T \hat{\mathbf{w}}_{n+1}$
 - 9: $\hat{\mathbf{v}}_{n+1} = \hat{\mathbf{v}}_{n+1} - V_n H_V(r : n, n)$, $\hat{\mathbf{w}}_{n+1} = \hat{\mathbf{w}}_{n+1} - W_n H_W(r : n, n - 1)$
 - 10: $H_V(n + 1, n) = \|\hat{\mathbf{v}}_{n+1}\|$, $H_W(n + 1, n - 1) = \|\hat{\mathbf{w}}_{n+1}\|$
 - 11: $\mathbf{v}_{n+1} = \hat{\mathbf{v}}_{n+1} / H_V(n + 1, n)$, $\mathbf{w}_{n+1} = \hat{\mathbf{w}}_{n+1} / H_W(n + 1, n - 1)$
 - 12: For reorthogonalization, **go to** line 4 and update H_V and H_W
 - 13: $\sigma_{n+1} = \mathbf{w}_{n+1}^T \mathbf{v}_{n+1}$
 - 14: **end for**
 - 15: Repeat lines 6, 7, 8 with $n = N$ to get $H_V(:, N)$, $H_W(:, N - 1)$, $H_W(:, N)$
-

If partial orthogonalization is used, the complexity is still $\mathcal{O}(N^2)$ as for Algorithm 1, both with and without reorthogonalization. If we use a full orthogonalization, the algorithm becomes much more expensive, yielding a cost of $\mathcal{O}(nN)$ at each step n , and therefore an overall complexity of $\mathcal{O}(N^3)$. However, the increased accuracy justifies the higher cost, as illustrated by the experiments in section 6.

4.3. Moment matrix formulation. To solve the IEP Problem 3.6, we look for nested biorthogonal subspaces for given vector spaces. Besides the block Krylov method as described before, these subspaces can be related to moment matrices.

The moment matrix $M_N \in \mathbb{R}^{N \times N}$, associated with two sets of vectors $X = \{\mathbf{x}_i\}_{i=1}^N$ and $Y = \{\mathbf{y}_i\}_{i=1}^N$ in vector spaces \mathcal{X} and \mathcal{Y} , respectively, is defined as

$$(28) \quad M_N = (\mathbf{y}_i^T \mathbf{x}_j)_{i,j=1}^N.$$

The following lemma states how to orthogonalize X and Y by factoring M_N .

Lemma 4.3 (Biorthonormal vectors via moment matrix factorization [13]). *Let $X = [\mathbf{x}_1 \ \mathbf{x}_2 \ \dots \ \mathbf{x}_N]$ and $Y = [\mathbf{y}_1 \ \mathbf{y}_2 \ \dots \ \mathbf{y}_N]$ be full-rank matrices in some vector spaces \mathcal{X} and \mathcal{Y} , respectively. Let M_N be the associated moment matrix 28. The (non-pivoted) LR factorization of M_N is given by $M_N = LR$, where L is a lower triangular matrix and R is an upper triangular matrix. Define*

$$V = [\mathbf{v}_1 \ \mathbf{v}_2 \ \dots \ \mathbf{v}_N] = XR^{-1}, \quad W = [\mathbf{w}_1 \ \mathbf{w}_2 \ \dots \ \mathbf{w}_N] = YL^{-T}.$$

Then, for $i = 1, \dots, N$, we have

$$\text{span}\{\mathbf{v}_1, \dots, \mathbf{v}_i\} = \text{span}\{\mathbf{x}_1, \dots, \mathbf{x}_i\},$$

$$\text{span}\{\mathbf{w}_1, \dots, \mathbf{w}_i\} = \text{span}\{\mathbf{y}_1, \dots, \mathbf{y}_i\},$$

and the vectors are biorthonormal

$$W^T V = L^{-1} M_N R^{-1} = I_N.$$

Consider $Z = \text{diag}(\{z_i\}_{i=1}^N)$ with distinct diagonal entries, and the matrices

$$K_V = [\mathbf{v}_1 \quad Z\mathbf{v}_1 \quad \dots \quad Z^{N-1}\mathbf{v}_1],$$

$$K_W = \begin{cases} \begin{bmatrix} \mathbf{w}_1 & \mathbf{w}_2 & Z\mathbf{w}_1 & Z\mathbf{w}_2 & \dots & Z^{k-1}\mathbf{w}_1 & Z^{k-1}\mathbf{w}_2 \end{bmatrix}, & \text{if } N = 2k, \\ \begin{bmatrix} \mathbf{w}_1 & \mathbf{w}_2 & Z\mathbf{w}_1 & Z\mathbf{w}_2 & \dots & Z^{k-1}\mathbf{w}_1 & Z^{k-1}\mathbf{w}_2 & Z^k\mathbf{w}_1 \end{bmatrix}, & \text{if } N = 2k + 1. \end{cases}$$

The columns of K_V and K_W form nested bases of the Krylov subspaces $\mathcal{K}_m(Z, \mathbf{v}_1)$ and $\mathcal{K}_m^\square(Z, [\mathbf{w}_1, \mathbf{w}_2])$, respectively, for all $m = 1, \dots, N$. Thus, we refer to the columns of K_V , K_W as Krylov bases. The moment matrix can now be constructed as $M_N = K_W^T K_V$, and it represents the moment matrix for a sequence of biorthonormal MOPs. A direct way to compute the recurrence coefficients of a set of biorthonormal MOPs is to evaluate the LR factorization of M_N . In finite precision, two issues are encountered with this procedure:

- The LR factorization without pivoting is numerically unstable,
- The matrix M_N tends to be very ill-conditioned.

The use of modified moments [17] could improve the conditioning of the moment matrix; however, we have not explored this approach in this setting.

5. CORE TRANSFORMATION ALGORITHM

This section presents an algorithm based on core transformations to solve the inverse eigenvalue problem described in Problem 3.6. The algorithm obtains the unique recurrence matrix H by applying a sequence of non-unitary similarity transformations⁶ $P_k^{-1} \dots P_1^{-1} Z P_1 \dots P_k$ on Z . These matrices P_i , called eliminators, are upper or lower triangular with a 2×2 active part acting on two consecutive rows or columns. More precisely, they are identity matrices with a

⁶In the literature, these transformations are typically referred to as core transformations [10].

2×2 lower or upper matrix, denoted by

$$(29) \quad \begin{bmatrix} & \\ \lrcorner & \end{bmatrix} = \begin{bmatrix} 1 & 0 \\ \tau & 1 \end{bmatrix} \quad \text{and} \quad \begin{bmatrix} & \\ \lrcorner & \end{bmatrix} = \begin{bmatrix} 1 & \tau \\ 0 & 1 \end{bmatrix},$$

embedded along the diagonal. This notation illustrates that a multiple of one row (or column) is added to the next or previous row (or column). For further reading on how eliminators can be used to solve inverse eigenvalue problems, we refer to [10, 27, 40]. Algorithm 3 provides an outline of the algorithm for a general dimension N . As for Algorithm 2, we use a MATLAB notation to denote the matrix entries. To illustrate the procedure, we consider an example with $N = 5$. We first do $N - 1$ steps which consist of three parts: *elimination*, *biorthogonalization* and *chasing*. By eliminating elements in $\mathbf{w}_1, \mathbf{w}_2$ and \mathbf{v}_1 using eliminators, condition (D1) will be satisfied. Hence, we need to find matrices W^{-1} and V^{-1} such that $W^{-1} [\mathbf{w}_1 \ \mathbf{w}_2] = [\mathbf{e}_1 \ \mathbf{e}_2]$ and $V^{-1} \mathbf{v}_1 = \mathbf{e}_1$. By using LU factorizations on the biorthogonalization step, we guarantee that Condition (D2) is satisfied. The matrices needed in the elimination and biorthogonalization steps are applied to the diagonal matrix Z . To achieve the desired banded structure (D3) of H , we perform a chasing step to remove undesired elements. At the end, we do a final N -th step to apply the appropriate scaling matrices.

Step 1. In the first step, the last element of \mathbf{w}_2 and \mathbf{v}_1 , as well as the last two elements of \mathbf{w}_1 are eliminated. More precisely, we compute eliminators $W_{2,5}^{-1}$, $W_{1,5}^{-1}$ and $W_{1,4}^{-1}$, where $W_{i,j}^{-1}$ is a lower eliminator that eliminates the j th-element of \mathbf{w}_i , i.e. the active part is a lower eliminator located in rows $j - 1$ and j . Also, a matrix $V_{1,5}^{-1}$ is needed to eliminate the last element in \mathbf{v}_1 . The total elimination matrices are $\widehat{W}_1^{-1} = W_{2,5}^{-1} W_{1,4}^{-1} W_{1,5}^{-1}$ and $\widehat{V}_1^{-1} = V_{1,5}^{-1}$. Applying these elimination matrices on the given vectors gives:

$$\widehat{W}_1^{-1} [\mathbf{w}_1 \ \mathbf{w}_2] = [\widehat{\mathbf{w}}_1 \ \widehat{\mathbf{w}}_2] \quad \text{and} \quad \widehat{V}_1^{-1} \mathbf{v}_1 = \widehat{\mathbf{v}}_1,$$

where the last element of $\widehat{\mathbf{v}}_1$ and $\widehat{\mathbf{w}}_2$ is zero, as well as the last two elements of $\widehat{\mathbf{w}}_1$. The elimination is depicted in Figure 1a, where the eliminators act on the vectors $\mathbf{w}_1, \mathbf{w}_2, \mathbf{v}_1$, and on the matrix Z . The eliminators on the left are applied to the left of Z , while those on the top are applied to the right. After the elimination step, we enforce biorthogonality as required by Condition (D2). This is achieved by setting $W_1 = \widehat{W}_1 L_1^T$ and $V_1 = \widehat{V}_1 U_1^{-1}$, where $(\widehat{W}_1)^T \widehat{V}_1 = L_1 U_1$ is an LU decomposition⁷. With this choice, the biorthogonality is satisfied:

$$W_1^T V_1 = L_1^{-1} \widehat{W}_1^T \widehat{V}_1 U_1^{-1} = L_1^{-1} (L_1 U_1) U_1^{-1} = I.$$

Accordingly, the transformed Z becomes

$$H^{(1)} = W_1^T Z V_1 = L_1^{-1} \widehat{W}_1^T Z \widehat{V}_1 U_1^{-1}.$$

It is essential that the biorthogonalization step preserves the zeros in $\mathbf{w}_1, \mathbf{w}_2, \mathbf{v}_1$ that were created in the previous steps. This is indeed the case as

$$\begin{aligned} W_1^{-1} [\mathbf{w}_1 \ \mathbf{w}_2] &= L_1^T \left(\widehat{W}_1^{-1} [\mathbf{w}_1 \ \mathbf{w}_2] \right) = L_1^T [\widehat{\mathbf{w}}_1 \ \widehat{\mathbf{w}}_2] = \begin{bmatrix} \mathbf{w}_1^{(1)} & \mathbf{w}_2^{(1)} \end{bmatrix}, \\ V_1^{-1} \mathbf{v}_1 &= U_1 \left(\widehat{V}_1^{-1} \mathbf{v}_1 \right) = U_1 \widehat{\mathbf{v}}_1 = \mathbf{v}_1^{(1)}, \end{aligned}$$

both retaining the created zeros since L_1^T and U_1 are upper triangular. As Z_1 has the desired bandwidth (14), no additional elimination steps on Z_1 , i.e., chasing, are necessary. The action of the operations on $\mathbf{w}_1, \mathbf{w}_2$, and \mathbf{v}_1 , along with the related operation on Z , is illustrated in Figure 1b. Note that only the eliminators \widehat{W}_1^{-1} and \widehat{V}_1^{-1} , indicated by arrow brackets, are

⁷We can not use a pivoted LU factorization. Hence, this a potential source for accuracy loss

Algorithm 3 IEP_CORE

Require: Diagonal matrix $Z = \text{diag}(z_1, \dots, z_N)$, vectors $\mathbf{w}_1, \mathbf{w}_2, \mathbf{v}_1 \in \mathbb{R}^N$ such that $\mathbf{w}_1^T \mathbf{v}_1 = 1$, $\mathbf{w}_2^T \mathbf{v}_1 = 0$ and $\mathbf{w}_2^T Z \mathbf{v}_1 = 1$.

Ensure: $W = [\mathbf{w}_1, \dots, \mathbf{w}_N]$, $V = [\mathbf{v}_1, \dots, \mathbf{v}_N] \in \mathbb{R}^{N \times N}$ such that $W^T V = I$, and H banded Hessenberg matrix as in (14) such that $W^T Z V = H$.

% Step 1

- 1: Compute eliminators $W_{1,N}^{-1}, W_{1,N-1}^{-1}, W_{2,N}^{-1}$ and $V_{1,N}^{-1}$
- 2: Compute $\widehat{W}_1^{-1} = W_{1,N}^{-1} W_{1,N-1}^{-1} W_{2,N}^{-1}$ and $\widehat{V}_1^{-1} = V_{1,N}^{-1}$
- 3: $\widehat{W}_1^T \widehat{V}_1 = L_1 U_1$
- 4: $W_1 = \widehat{W}_1 L_1^{-1}$ and $V_1 = \widehat{V}_1 U_1^{-1}$
- 5: $W^T = W_1, V = V_1$ and $H^{(1)} = W^T Z V$

% Step 2 to $N - 2$

- 6: **for** $i = 2 : N - 2$ **do**
- 7: Compute eliminators $W_{1,N-i}, W_{2,N-i-1}$ and $V_{1,N-i-1}$
- 8: $\widehat{W}_i = W_{1,N-i} W_{2,N-i-1}$ and $\widehat{V}_i = V_{1,N-i-1}$
- 9: $\widehat{W}_i^T \widehat{V}_i = L_i U_i$
- 10: $W_i = \widehat{W}_i L_i^{-T}$ and $V_i = \widehat{V}_i U_i^{-1}$
- 11: $W^T = W_i^T W^T, V = V V_i, H^{(i)} = W_i^T H^{(i-1)} V_i$
- 12: **for** $j = 0 : i - 1$ **do**
- 13: Eliminate $H^{(i)}(N - i + j + 1, N - i + j)$ **% Chase lower bulge**
- 14: Eliminate $H^{(i)}(N - i + j - 1, N - i + j + 2)$ **% Chase upper bulge**
- 15: **end for**
- 16: **end for**

% Step $N - 1$

- 17: Compute W_{N-1}^T and $V_{N-1} = W_{N-1}^{-1}$
- 18: $W^T = W_{N-1}^T W^T, V = V V_{N-1}, H^{(N-1)} = W_{N-1}^T H^{(N-2)} V_{N-1}$
- 19: **for** $j = 0 : (N-3)$ **do**
- 20: Eliminate $H^{(N-1)}(j + 3, j + 1)$ **% Chase lower bulge**
- 21: **end for**

% Step N

- 22: Apply S_1, S_2, S_3 such that $\mathbf{e}_1 = S_1 \mathbf{w}_1^{(N-1)}, \mathbf{e}_2 = S_2 \mathbf{w}_2^{(N-1)}$ and $\mathbf{e}_1 = S_3 \mathbf{v}_1^{(N-1)}$
- 23: Apply scaling W_s such that lower diagonal of $H^{(N)} = W_s H^{(N-1)} W_s^{-1}$ are all ones

shown. The matrices L_1 and U_1 , used in the biorthogonalization, are omitted to avoid an overly complicated visual representation. Nevertheless, their action on Z and the vectors \mathbf{w}_1 , \mathbf{w}_2 , and \mathbf{v}_1 is always illustrated.

Step 2. The result after the elimination and biorthogonalization of step 2 is illustrated in Figure 1c. The elimination differs slightly from step 1 as we only remove one element from $\mathbf{w}_1^{(1)}$ instead of two elements as in the previous step. More precisely, we apply $\widehat{W}_2^{-1} = W_{2,4}^{-1} W_{1,3}^{-1}$ and $\widehat{V}_2^{-1} = V_{1,4}^{-1}$:

$$\widehat{W}_2^{-1} \begin{bmatrix} \mathbf{w}_1^{(1)} & \mathbf{w}_2^{(1)} \end{bmatrix} = \begin{bmatrix} \widehat{\mathbf{w}}_1^{(1)} & \widehat{\mathbf{w}}_2^{(1)} \end{bmatrix} \quad \text{and} \quad \widehat{V}_2^{-1} \mathbf{v}_1^{(1)} = \widehat{\mathbf{v}}_1^{(1)},$$

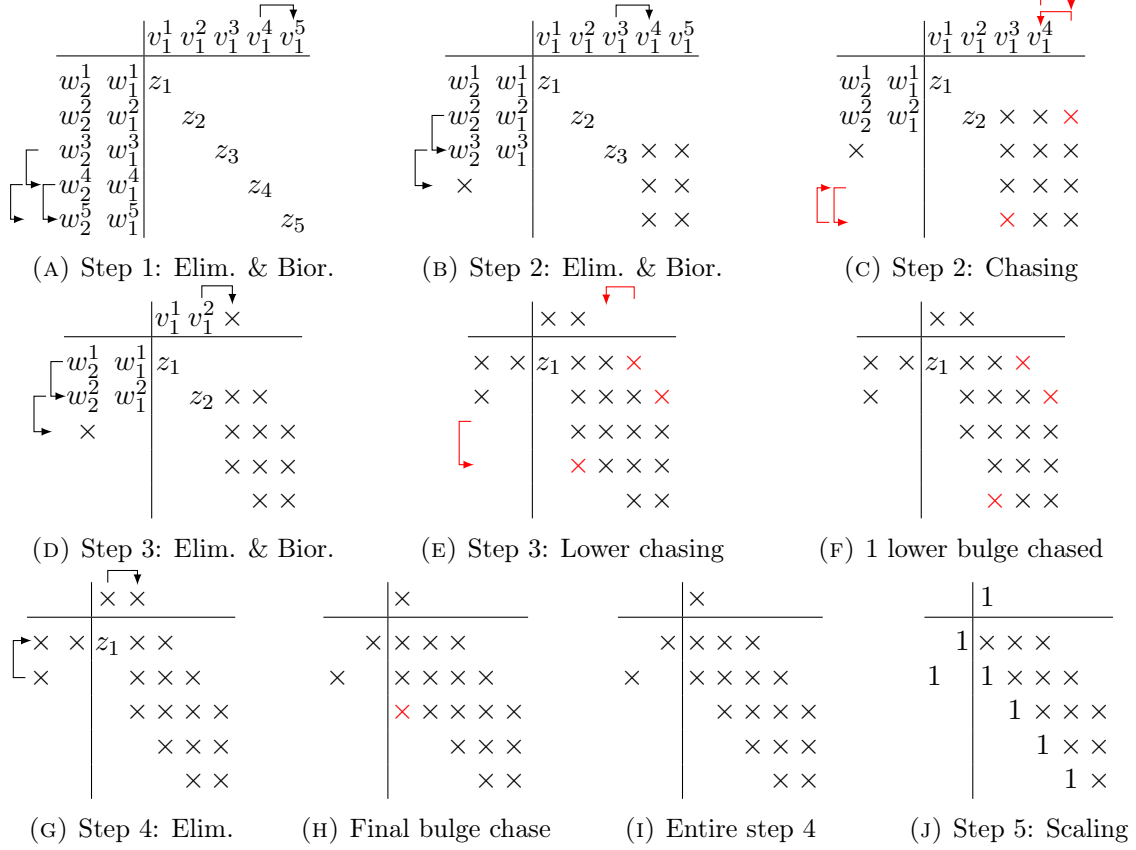


FIGURE 1. Visualization of different steps in Algorithm 3 for $N = 5$. To simplify the notation, we do not display the transformations for the biorthogonalization.

where the last two elements of $\hat{\mathbf{v}}_1^{(1)}$ and $\hat{\mathbf{w}}_2^{(1)}$ are zero, as well as the last three elements of $\hat{\mathbf{w}}_1^{(1)}$. Performing another LU decomposition gives the relations $W_2 = \hat{W}_2 L_2^{-T}$ and $V_2 = \hat{V}_2 U_2^{-1}$, ensuring that $W_2^T V_2 = I$. Applying W_2 and V_2 to the vectors results in

$$W_2^{-1} \begin{bmatrix} \mathbf{w}_1^{(1)} & \mathbf{w}_2^{(1)} \end{bmatrix} = L_2^T \left(\hat{W}_2^{-1} \begin{bmatrix} \mathbf{w}_1^{(1)} & \mathbf{w}_2^{(1)} \end{bmatrix} \right) = L_2^T \begin{bmatrix} \hat{\mathbf{w}}_1^{(1)} & \hat{\mathbf{w}}_2^{(1)} \end{bmatrix} = \begin{bmatrix} \mathbf{w}_1^{(2)} & \mathbf{w}_2^{(2)} \end{bmatrix},$$

$$V_2^{-1} \mathbf{v}_1^{(1)} = U_2 \left(\hat{V}_2^{-1} \mathbf{v}_1^{(1)} \right) = U_2 \hat{\mathbf{v}}_1^{(1)} = \mathbf{v}_1^{(2)},$$

again retaining the desired zeros. A second difference is that $\tilde{H}^{(2)} = W_2^T H^{(1)} V_2$ has two unwanted elements which are indicated by red crosses in Figure 1c. We will refer to these unwanted elements as the *bulges*. A chasing step has to be done to eliminate these bulges. The lower bulges, which are unwanted elements on the lower diagonal, are removed with an appropriate lower eliminator $W_{2,1}$ acting on the last two rows of $\tilde{H}^{(2)}$. Since we must have a similarity transformation, we apply $W_{2,1}^{-1}$ on the right side of $\tilde{H}^{(2)}$. A similar step with an upper eliminator $V_{2,1}$ acting on the last two columns of $\tilde{H}^{(2)}$ is done to eliminate the element in the upper bulge. The transformation $H^{(2)} = V_{2,1}^{-1} W_{2,1} \tilde{H}^{(2)} W_{2,1}^{-1} V_{2,1}$, shown in Figure 1c, removes the unwanted elements in $\tilde{H}^{(2)}$. One can easily see that these eliminators in the chasing steps do not destroy the created zeros in $\mathbf{w}_1^{(2)}$ and $\mathbf{w}_2^{(2)}$.

Step 3. The elimination and biorthogonalization of step 3 are similar to the previous step, yielding $\tilde{H}^{(3)} = W_3^T H^{(2)} V_3$. In Figure 1e, one can see that the bulge now consists of 2 upper elements and 1 lower element. The chasing procedure now becomes a bit more technical. The chasing step is illustrated for the lower bulges, as the process for the upper bulges is analogous. As depicted with the red arrow, one can eliminate the lower bulges by a lower eliminator $W_{3,1}$ acting on the left of $\tilde{H}^{(4)}$. To enforce biorthogonality, we apply the inverse on the right, resulting in $W_{3,1} \tilde{H}^{(4)} W_{3,1}^{-1}$ which is shown in Figure 1f. Now, the biorthogonality constraint introduced a new lower bulge, positioned in the last row. Because of this bulge movement, this step is commonly referred to as *bulge chasing* (see, e.g., [19, Chapter 7]). The lower-positioned bulge can be removed by a transformation similar to the chasing part of step 2. Figure 1g shows the situation after the entire chasing procedure. In general, in the chasing step of step i where $1 < i < N - 1$, we perform $(i - 1)$ eliminations in both the lower and upper part of the matrix.

Step 4. The penultimate step is special, as we use an upper eliminators to create the necessary zeros, instead of relying on lower eliminators. More specifically, take W_4^{-1} as an upper eliminator such that $W_4^{-1} \mathbf{w}_2^{(3)} = c \mathbf{e}_2$, where c is a nonzero constant; i.e., the first element of $\mathbf{w}_2^{(3)}$ is eliminated. We also need to eliminate the second element in $\mathbf{v}_1^{(3)}$ in this step; see Figure 1g. It turns out that $V_4^{-1} = W_4^T$ can be used for this, which at the same time ensures the biorthogonality condition for this step. To see why this choice is justified, we note that during all steps, the orthogonality of $\mathbf{v}_1^{(k)}$ and $\mathbf{w}_2^{(k)}$ is preserved. In particular,

$$0 = \left(\mathbf{w}_2^{(4)} \right)^T \mathbf{v}_1^{(4)} = \left(W_4^{-1} \mathbf{w}_2^{(3)} \right)^T \left(W_4^T \mathbf{v}_1^{(3)} \right) = c \mathbf{e}_2^T \left(W_4^T \mathbf{v}_1^{(3)} \right).$$

Thus, the second element of $W_4^T \mathbf{v}_1^{(3)}$ is eliminated as c is not zero. From Figure 1h, it can be seen that $\tilde{H}^{(4)} = W_4^T H^{(3)} V_4$ still has one lower bulge element. To complete Step 4, a lower bulge-chasing step is required to obtain the configuration shown in Figure 1i.

Step 5. The last part of the algorithm applies appropriate *scaling* matrices. We apply matrices S_1, S_2, S_3 such that $S_1 \mathbf{w}_1^{(4)} = \mathbf{e}_1$, $S_2 \mathbf{w}_2^{(4)} = \mathbf{e}_2$ and $S_3 \mathbf{v}_1^{(4)} = \mathbf{e}_1$; see Figure 1j. Recall from the initial conditions that we have $\mathbf{w}_2^T Z \mathbf{v}_1 = 1$. At this stage of the algorithm, we satisfy condition Figure (D1), and thus

$$\mathbf{e}_2^T H^{(4)} \mathbf{e}_1 = \mathbf{e}_2^T W_5^T Z V_5 \mathbf{e}_1 = \mathbf{w}_2^T Z \mathbf{v}_1 = 1.$$

The second scaling step applies a similarity transformation on $H^{(5)}$ such that all elements on the subdiagonal are one. To this end, we compute $H^{(5)} = D_s H^{(4)} D_s^{-1}$ with

$$(30) \quad D_s = \text{diag} \left(1, 1, \frac{1}{H^{(4)}(3, 2)}, \frac{1}{H^{(4)}(3, 2)H^{(4)}(4, 3)}, \frac{1}{H^{(4)}(3, 2)H^{(4)}(4, 3)H^{(4)}(5, 4)} \right).$$

Remark 5.1. Similar to Algorithm 2, we chose not to apply this scaling to the basis vectors W and V , as it is an ill-conditioned transformation due to the typically large magnitude variation of the entries in D_s .

6. NUMERICAL EXPERIMENTS

In this section, we compare our numerical algorithms with the explicit formulae given by Arvesú, Coussement, and Van Assche [7] for the recurrence matrix associated with two examples of discrete multiple orthogonal polynomials, namely the Kravchuk and Hahn MOPs. In section 6.2, we illustrate — using the multi-precision computing toolbox Advanpix in MATLAB

— that the IEP linked to these Kravchuk and Hahn polynomials is ill-conditioned. Furthermore, we also investigate the stability of our algorithms. Finally, we consider IEPs which are better conditioned than the ones related to Kravchuk and Hahn MOPs to illustrate that our algorithms perform well. All MATLAB codes are publicly available⁸.

6.1. Kravchuk and Hahn Multiple Orthogonal Polynomials. Arvesú et al. [7] gave explicit expressions for certain discrete multiple orthogonal polynomials and their recurrence coefficients. These examples include Charlier, Meixner, Kravchuk and Hahn MOPs. We tested Hahn and Kravchuk MOPs, as our setting assumes finitely many nodes in the discrete measures. The measures corresponding to these MOPs are examples of AT systems for the case $r = 2$ (cf. [7]).

Example 1: Multiple Kravchuk polynomials. Kravchuk polynomials arise when the discrete measures are binomial distributions on the integers. More concretely,

$$\mu_j = \sum_{i=0}^{N-1} p_j^i (1-p_j)^{N-i} \delta_i, \quad j \in \{1, 2\},$$

where $0 < p_j < 1$ are all distinct. We use $p_1 = 0.4$ and $p_2 = 0.5$ in all our experiments. Explicit formulae for the type II multiple Kravchuk polynomials $K_{n_1, n_2}^{p_1, p_2, N}(x)$ can be derived. This is done by defining a suitable *raising operator* and corresponding *Rodrigues formula* [7, Sec. 4.4]. For the multi-index (n_1, n_2) , one obtains

$$K_{n_1, n_2}^{p_1, p_2, N}(x) = p_1^{n_1} p_2^{n_2} (-N-1)_{n_1+n_2} \sum_{j=0}^{n_1+n_2} \sum_{k=0}^j \frac{(-n_1)_k}{k!} \left(\frac{1}{p_1}\right)^k \frac{(-n_2)_{j-k}}{(j-k)!} \left(\frac{1}{p_2}\right)^{j-k} \frac{(-x)_j}{(-N-1)_j},$$

where $(c)_j$ denotes the Pochhammer function of c , given by $(c)_j = \prod_{i=0}^{j-1} (c+i)$ for $j > 0$, and $(c)_0 = 1$.

Example 2: Multiple Hahn polynomials. We obtain Hahn polynomials when we take hypergeometric distributions on the integers as measures. We get

$$\mu_j = \sum_{i=0}^{N-1} \frac{(\beta_j + 1)_i}{i!} \frac{(\gamma + 1)_{N-i-1}}{(N-1-i)!} \delta_i, \quad \beta_j > -1, \quad \gamma > -1, \quad j \in \{1, 2\},$$

with all β_j distinct. We use $\beta_1 = 1$, $\beta_2 = 1.5$ and $\gamma = 1$ in all our experiments. Also, for this AT system, one can find explicit formulae [7].

We compare our algorithms by computing the forward relative error

$$(31) \quad e_N = \frac{\|H_N - \hat{H}_N\|_2}{\|H_N\|_2}$$

where \hat{H}_N is the numerically obtained solution and H_N is the exact solution [7]. In Figure 2, we show the forward relative error e_N and the loss of biorthogonality $\|I_N - W^T V\|_2$, plotted over dimensions $N = 5, \dots, 30$ for the Kravchuk and Hahn MOPs. From this, we can draw a couple of observations. The forward relative error e_N has similar growth for IEP_CORE and IEP_KRYLREORTH(full), while the error is larger for IEP_KRYL. As explained in previous sections, the bases W and V for IEP_KRYL correspond to monic type

⁸<https://gitlab.kuleuven.be/numa/public/IEP-MOP>

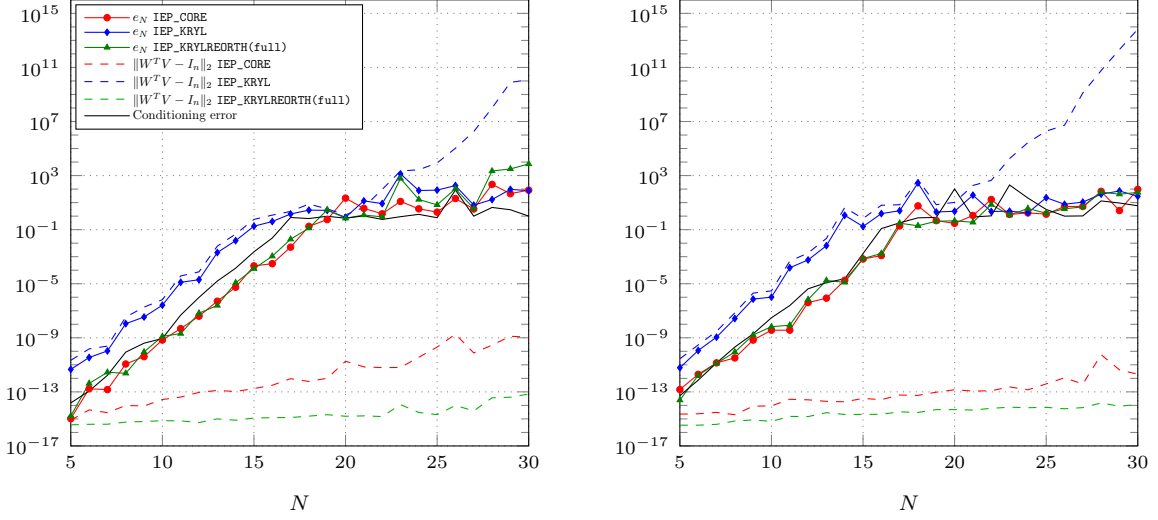


FIGURE 2. Accuracy and biorthogonalization loss of the various algorithms for the Kravchuk (left) and Hahn (right) MOPs.

II MOPs which are ill-conditioned. In contrast, we do not scale W and V for `IEP_CORE` and `IEP_KRYLREORTH(full)` in order to have a better conditioned basis, and thus they are diagonal scalings of the basis vectors connected to monic type II MOPs. The loss of biorthogonality for `IEP_CORE` and `IEP_KRYLREORTH(full)` remains small with increasing dimension, while it increases exponentially for the ill-conditioned basis vectors in `IEP_KRYL`. In Figure 3, the distance between H_{20} and the numerical solution \hat{H}_{20} for the different diagonals, computed with `IEP_KRYLREORTH(full)`, is visualized. Although the initial columns of H_N are approximated with high precision, the error increases exponentially as the column index grows. The problems appear to be highly ill-conditioned as it will be analyzed in more detail in the next section.

6.2. Conditioning and stability. The errors in Figure 2 show that for values of N between 15 and 20, all decimal digits of precision for the entries in \hat{H}_N are lost. This loss may be attributed either to instability of the methods or to ill-conditioning of the underlying problem. To investigate this, we examine the conditioning of the problem where the input consists of the nodes z_i and the weights $\alpha_{j,i}$ of the two discrete measures, and the output is the banded Hessenberg matrix H_N . Given this input, we compute the matrix H_N in quadruple precision using the Advanpix Multiprecision Computing Toolbox⁹. Next, we perturb the input data with relative errors on the order of machine precision and compute the solution of the problem \hat{H}_N in quadruple precision. The relative difference between H_N and \hat{H}_N , shown as the black line in Figure 2, represents the conditioning error. The forward relative errors e_N are of the same order of magnitude as the conditioning error, indicating that all algorithms are weakly stable for this problem.

To assess the backward stability we check if the computed solution \hat{H}_N corresponds to the exact solution of slightly perturbed input data \hat{z}_i and $\hat{\alpha}_{j,i}$ where the relative perturbation is of the size of the machine precision. As for the conditioning and the forward error, we

⁹<https://www.advanpix.com/>

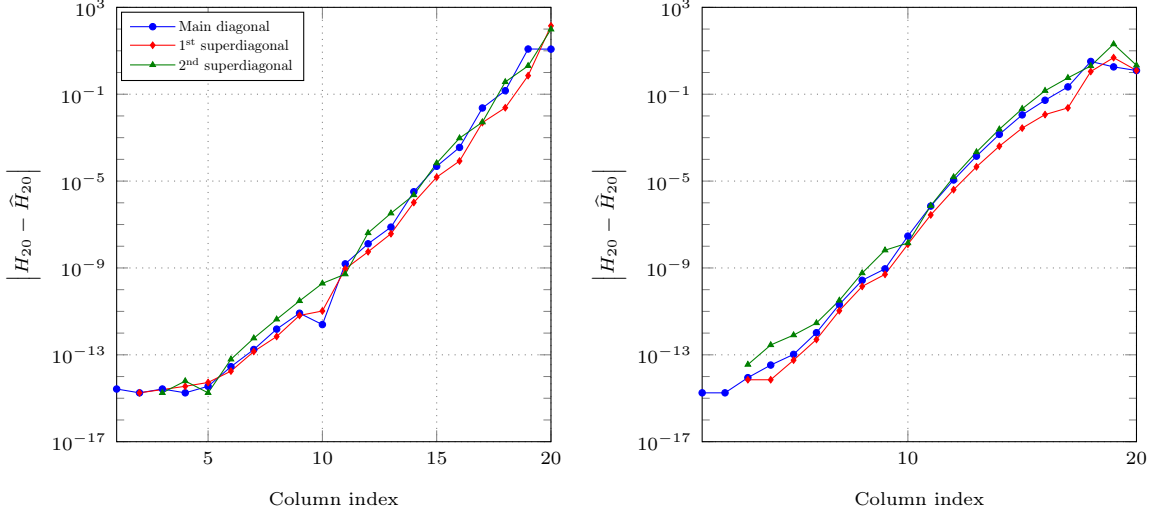


FIGURE 3. accuracy $|H_{20} - \hat{H}_{20}|$ of `IEP_KRYLREORTH(full)` for Kravchuk MOPs (left) and Hahn MOPs (right).

approximate computing in exact arithmetic by performing the computations in quadruple precision. Figure 4 shows the relative backward errors on the vector of nodes \mathbf{z} and the two weight vectors α_1 and α_2 in function of the dimension N for the three algorithms. The problem considered is the computation of the recurrence coefficients for multiple Hahn polynomials with the same parameters as before. The results presented in the figure indicate that `IEP_CORE` and `IEP_KRYLREORTH(full)` exhibit backward stability for most values of $N < 25$. For $N \geq 25$, backward instability is observed for both methods. In contrast, `IEP_KRYL` is not backward stable for any of the considered values of N .

6.3. Other IEPs. In this section, we solve other IEPs which are better conditioned than the Kravchuk and Hahn examples. Although we don't have the explicit formulae for the recurrence coefficients of these examples, we approximate the exact solution using quadruple precision with Advanpix. This approximated exact recurrence matrix is denoted by H_N and the numerical approximation using double precision with \hat{H}_N . Similar as in section 6.1, we compare the algorithms by using the forward relative error e_N (31) and loss of biorthogonality. Note that the examples below are not guaranteed to be AT-systems. Nevertheless, we numerically verified the rank of the moment matrix (see equation (3)) to ensure a normal index, which guarantees the existence of a unique set of MOPs.

- **Equidistant nodes in $[-1,1]$ and random weights $\alpha_j \sim \mathcal{U}(1,2)^N$:**

$\mathcal{U}(a,b)$ denotes the uniform distribution on the interval (a,b) . The results in Figure 5 indicate that the reorthogonalized version `IEP_KRYLREORTH(full)` outperforms `IEP_KRYLOV`. In contrast, the error associated with `IEP_CORE` appears to be highly sensitive to the randomness in the weights. A sudden increase in the loss of biorthogonality is observed for `IEP_CORE` around $N = 60$. This phenomenon can be attributed to the significant increase in the magnitude of τ in the eliminators equation (29) as N increases, with values ranging approximately from 10^4 to 10^{10} .

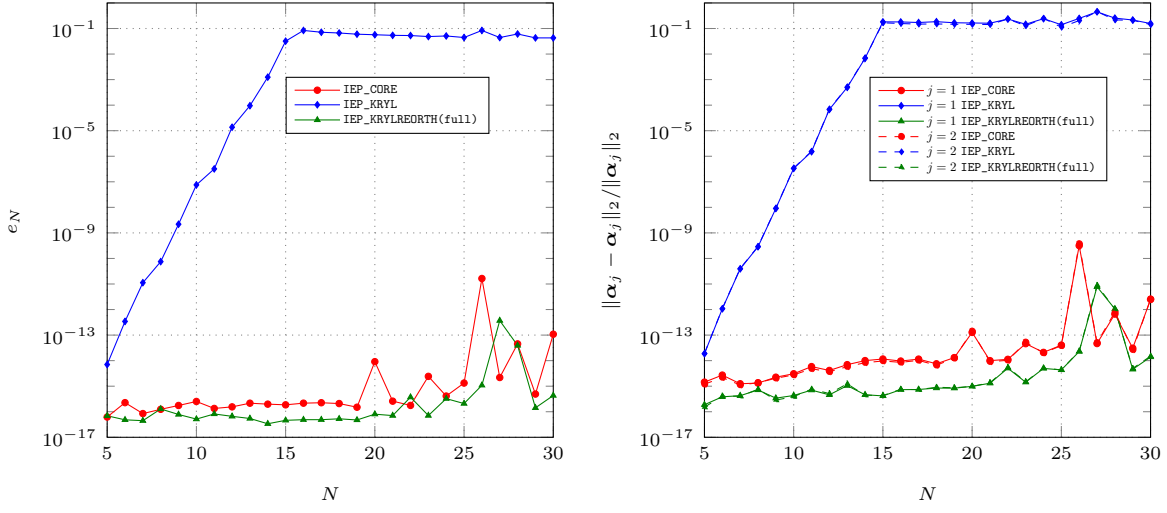


FIGURE 4. Comparison of backward error on nodes (left) and weights (right) for multiple Hahn polynomials. Note that the dashed lines in the right figure almost coincide with the solid lines.

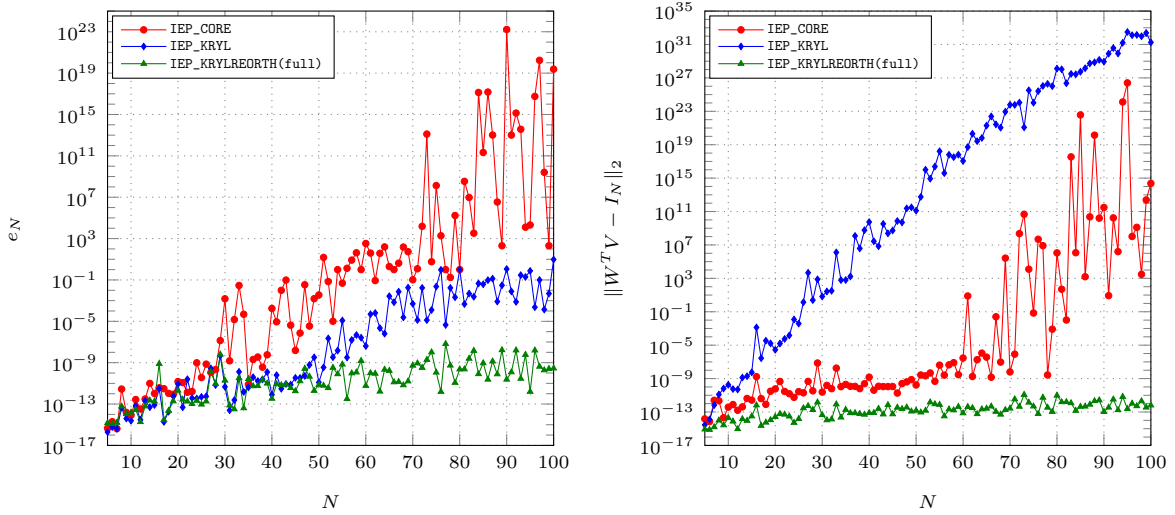


FIGURE 5. Error comparison (left) and loss of biorthogonality (right) for equidistant nodes in $[-1, 1]$ and random weights.

- **Chebyshev nodes in $[-1, 1]$ and random weights $\alpha_j \sim \mathcal{U}(1, 2)^N$:**

Due to the good approximation properties of Chebyshev nodes, one would expect that this gives a better-conditioned inverse eigenvalue problem. This explains why in Figure 6, IEP_KRYL and IEP_KRYLREORTH(full) have similar performance for this choice of nodes and weights. Both Krylov methods clearly outperform IEP_CORE.

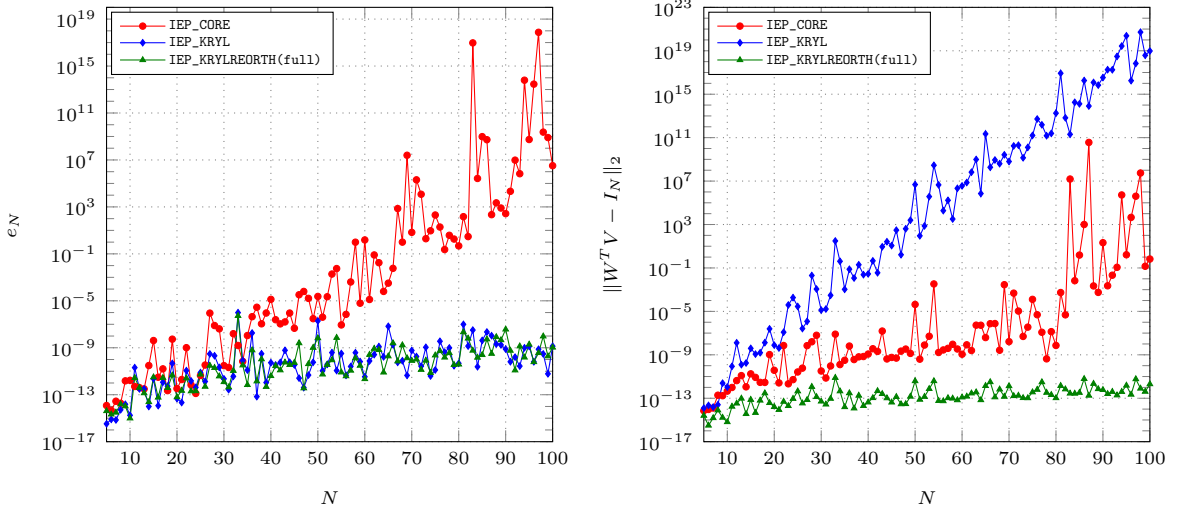


FIGURE 6. Error comparison (left) and loss of biorthogonality (right) for Chebyshev nodes in $[-1, 1]$ and random weights.

In a final experiment, illustrated in Figure 7, the precision of the Krylov-based algorithms is compared for higher values of N . More precisely, `IEP_KRYLREORTH(full)`, `IEP_KRYLREORTH(partial)` and `IEP_KRYL` are compared using the nodes and weights described above. For the well-conditioned Chebyshev example, all three methods exhibit comparable performance, with a relative forward error e_N of approximately 10^{-4} at $N = 1000$. In contrast, for the case with equidistant nodes in the interval $[-1, 1]$, the benefits of full reorthogonalization become apparent. While `IEP_KRYL` and `IEP_KRYLREORTH(partial)` have acceptable accuracy up to $N = 50$, the fully reorthogonalized variant `IEP_KRYLREORTH(full)` extends this limit to $N = 150$ for a similar level of relative error.

7. CONCLUSION

By connecting MOPs, Krylov subspaces and inverse eigenvalue problems, we derive a Krylov-based method and a core transformation algorithm to compute the unique recurrence coefficients associated with the MOPs on the step-line. The methods `IEP_CORE` and `IEP_KRYLREORTH(full)` have similar performance for the ill-conditioned examples associated with Hahn and Kravchuk. However, the experiments on better-conditioned problems show that `IEP_KRYLREORTH(full)` achieves the highest accuracy and overall best performance among the methods considered, at the price of a higher computational cost. A theoretical analysis of the numerical properties of the IEP could provide more insight, for example, on the conditioning of the problem. Furthermore, an updating/downdating approach can be applied as well, which has proven to be more flexible as it allows reusing the existing recurrence relations to build new recurrences under modest modifications, such as adding or deleting nodes of the inner product [21, 28, 33, 39, 41, 43]. A natural direction for future research is the generalization towards other recurrence relations for MOPs such as the nearest-neighbor recurrence relations [36]. Finally, it would be interesting to compare our methods with the techniques in [14, 29].

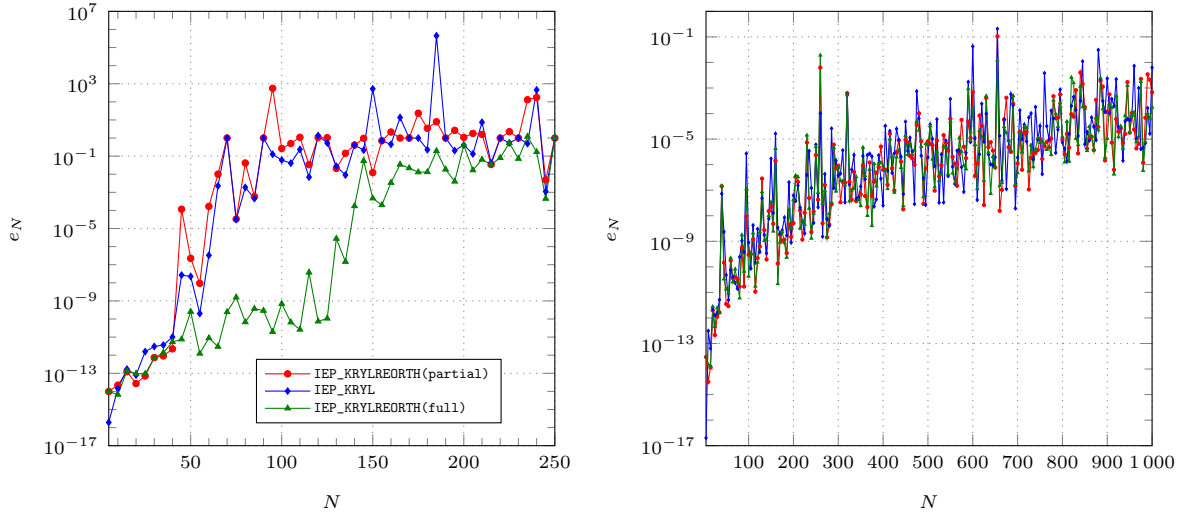


FIGURE 7. Error comparison for equidistant nodes in $[-1,1]$ and uniform random weights (left) and Chebyshev nodes in $[-1,1]$ and uniform random weights (right) for larger values of N

FUNDING

The research was partially supported by the Research Council KU Leuven (Belgium), project C16/21/002 (Manifactor: Factor Analysis for Maps into Manifolds) and by the Fund for Scientific Research – Flanders (Belgium), projects G0A9923N (Low rank tensor approximation techniques for up- and downdating of massive online time series clustering) and G0B0123N (Short recurrence relations for rational Krylov and orthogonal rational functions inspired by modified moments), and junior postdoctoral fellowship 12A1325N (Short Recurrences for Block Krylov Methods with Applications to Matrix Functions and Model Order Reduction) for the second author.

REFERENCES

- [1] J. I. ALIAGA, D. L. BOLEY, R. W. FREUND, AND V. HERNÁNDEZ, *A Lanczos-type method for multiple starting vectors*, Math. Comp., 69 (2000), pp. 1577–1601.
- [2] H. ALQAHTANI AND L. REICHEL, *Multiple orthogonal polynomials applied to matrix function evaluation*, BIT, 58 (2018), pp. 835–849.
- [3] A. APTEKAREV AND V. KALIAGUINE, *Complex rational approximation and difference operators*, in Proceedings of the Third International Conference on Functional Analysis and Approximation Theory, Vol. I (Acquafredda di Maratea, 1996), no. 52 in Suppl. Rend. Circ. Matem. Palermo, Ser. II, 1998, pp. 3–21.
- [4] A. I. APTEKAREV, *Multiple orthogonal polynomials*, J. Comput. Appl. Math., 99 (1998), pp. 423–447.
- [5] —, *Spectral problems of high-order recurrences*, in Spectral theory and differential equations, vol. 233 of Amer. Math. Soc. Transl. Ser. 2, Amer. Math. Soc., Providence, RI, 2014, pp. 43–61.
- [6] A. I. APTEKAREV, F. MARCELLÁN, AND I. A. ROCHA, *Semiclassical multiple orthogonal polynomials and the properties of Jacobi-Bessel polynomials*, J. Approx. Theory, 90 (1997), pp. 117–146.
- [7] J. ARVESÚ, J. COUSSEMENT, AND W. VAN ASSCHE, *Some discrete multiple orthogonal polynomials*, in Proceedings of the Sixth International Symposium on Orthogonal Polynomials, Special Functions and their Applications (Rome, 2001), vol. 153, 2003, pp. 19–45.

- [8] D. BOLEY AND G. H. GOLUB, *A survey of matrix inverse eigenvalue problems*, Inverse Problems, 3 (1987), pp. 595–622.
- [9] C. F. BORGES, *On a class of Gauss-like quadrature rules*, Numer. Math., 67 (1994), pp. 271–288.
- [10] D. CAMPS, K. MEERBERGEN, AND R. VANDEBRIL, *An implicit filter for rational Krylov using core transformations*, Linear Algebra Appl., 561 (2019), pp. 113–140.
- [11] M. T. CHU, *Inverse eigenvalue problems*, SIAM Rev., 40 (1998), pp. 1–39.
- [12] J. COUSSEMENT AND W. VAN ASSCHE, *Gaussian quadrature for multiple orthogonal polynomials*, J. Comput. Appl. Math., 178 (2005), pp. 131–145.
- [13] P. J. DAVIS, *Interpolation and Approximation*, Blaisdell Publishing Co. [Ginn and Co.], New York-Toronto-London, 1963.
- [14] G. FILIPUK, M. HANECZOK, AND W. VAN ASSCHE, *Computing recurrence coefficients of multiple orthogonal polynomials*, Numer. Algorithms, 70 (2015), pp. 519–543.
- [15] R. W. FREUND, *The look-ahead Lanczos process for nonsymmetric matrices and its applications*, in Proceedings of the Cornelius Lanczos International Centenary Conference (Raleigh, NC, 1993), SIAM, Philadelphia, PA, 1994, pp. 33–47.
- [16] A. FROMMER, K. LUND, AND D. B. SZYLD, *Block Krylov subspace methods for functions of matrices*, Electron. Trans. Numer. Anal., 47 (2017), pp. 100–126.
- [17] W. GAUTSCHI, *Orthogonal Polynomials: Computation and Approximation*, Oxford University Press, 04 2004.
- [18] G. H. GOLUB AND G. MEURANT, *Matrices, Moments and Quadrature with Applications*, Princeton Series in Applied Mathematics, Princeton University Press, Princeton, NJ, 2010.
- [19] G. H. GOLUB AND C. F. VAN LOAN, *Matrix Computations*, Johns Hopkins Studies in the Mathematical Sciences, Johns Hopkins University Press, Baltimore, MD, fourth ed., 2013.
- [20] G. H. GOLUB AND J. H. WELSCH, *Calculation of Gauss quadrature rules*, Math. Comp., 23 (1969), pp. 221–230.
- [21] W. B. GRAGG AND W. J. HARROD, *The numerically stable reconstruction of Jacobi matrices from spectral data*, Numer. Math., 44 (1984), pp. 317–335.
- [22] M. E. H. ISMAIL, *Classical and Quantum Orthogonal Polynomials in One Variable*, vol. 98 of Encyclopedia of Mathematics and its Applications, Cambridge University Press, Cambridge, 2005.
- [23] A. B. J. KUIJLAARS, *Multiple orthogonal polynomials in random matrix theory*, in Proceedings of the International Congress of Mathematicians. Volume III, Hindustan Book Agency, New Delhi, 2010, pp. 1417–1432.
- [24] T. LAUDADIO, N. MASTRONARDI, W. VAN ASSCHE, AND P. VAN DOOREN, *A Matlab package computing simultaneous Gaussian quadrature rules for multiple orthogonal polynomials*, J. Comput. Appl. Math., 451 (2024), pp. Paper No. 116109, 17.
- [25] T. LAUDADIO, N. MASTRONARDI, AND P. VAN DOOREN, *Computational aspects of simultaneous Gaussian quadrature*, Numer. Algor., (2024).
- [26] K. LUND, *A New Block Krylov Subspace Framework with Applications to Functions of Matrices Acting on Multiple Vectors*, ProQuest LLC, Ann Arbor, MI, 2018. Thesis (Ph.D.)—Temple University.
- [27] T. MACH, M. VAN BAREL, AND R. VANDEBRIL, *Inverse eigenvalue problems for extended Hessenberg and extended tridiagonal matrices*, J. Comput. Appl. Math., 272 (2014), pp. 377–398.
- [28] N. MASTRONARDI AND P. VAN DOOREN, *The QR steps with perfect shifts*, SIAM J. Matrix Anal. Appl., 39 (2018), pp. 1591–1615.
- [29] G. V. MILOVANOVIĆ AND M. STANIĆ, *Construction of multiple orthogonal polynomials by discretized Stieltjes-Gautschi procedure and corresponding Gaussian quadratures*, Facta Univ. Ser. Math. Inform., (2003), pp. 9–29.
- [30] J. MÍNGUEZ CENICEROS AND W. VAN ASSCHE, *Multiple orthogonal polynomials on the unit circle*, Constr. Approx., 28 (2008), pp. 173–197.
- [31] R. B. MORGAN AND D. A. NICELY, *Restarting the nonsymmetric Lanczos algorithm for eigenvalues and linear equations including multiple right-hand sides*, SIAM J. Sci. Comput., 33 (2011), pp. 3037–3056.
- [32] Multiprecision Computing Toolbox for MATLAB, Advanpix LLC., Yokohama, Japan, (2015).
- [33] H. RUTISHAUSER, *On Jacobi rotation patterns*, in Experimental Arithmetic, High Speed Computing and Mathematics. Proceedings of Symposia in Applied Mathematics, vol. 15 of Proceedings of Symposia in Applied Mathematics, Amer. Math. Soc., Providence, RI, 1963, pp. 219–239.
- [34] Y. SAAD, *Iterative Methods for Sparse Linear Systems*, Society for Industrial and Applied Mathematics, Philadelphia, PA, second ed., 2003.

- [35] W. VAN ASSCHE, *Padé and Hermite-Padé approximation and orthogonality*, Surv. Approx. Theory, 2 (2006), pp. 61–91.
- [36] ———, *Nearest neighbor recurrence relations for multiple orthogonal polynomials*, J. Approx. Theory, 163 (2011), pp. 1427–1448.
- [37] ———, *A Golub-Welsch version for simultaneous gaussian quadrature*, Numer. Algor., (2024).
- [38] W. VAN ASSCHE AND E. COUSSEMENT, *Some classical multiple orthogonal polynomials*, J. Comput. Appl. Math., 127 (2001), pp. 317–347.
- [39] M. VAN BAREL, N. VAN BUGGENHOUT, AND R. VANDEBRIL, *Algorithms for modifying recurrence relations of orthogonal polynomial and rational functions when changing the discrete inner product*, Appl. Numer. Math., 200 (2024), pp. 429–452.
- [40] N. VAN BUGGENHOUT, *Structured Matrix Techniques for Orthogonal Rational Functions and Rational Krylov Methods*, PhD thesis, KU Leuven, 2021.
- [41] ———, *On generating Sobolev orthogonal polynomials*, Numer. Math., 155 (2023), pp. 415–443.
- [42] N. VAN BUGGENHOUT, M. VAN BAREL, AND R. VANDEBRIL, *Biorthogonal rational Krylov subspace methods*, Electron. Trans. Numer. Anal., 51 (2019), pp. 451–468.
- [43] ———, *Generation of orthogonal rational functions by procedures for structured matrices*, Numer. Algor., 89 (2022), pp. 551–582.

NUMERICAL ANALYSIS AND APPLIED MATHEMATICS (NUMA) UNIT, DEPARTMENT OF COMPUTER SCIENCE, KU LEUVEN, LEUVEN, BELGIUM.

Email address: `amin.faghih@kuleuven.be`

NUMERICAL ANALYSIS AND APPLIED MATHEMATICS (NUMA) UNIT, DEPARTMENT OF COMPUTER SCIENCE, KU LEUVEN, LEUVEN, BELGIUM.

Email address: `michele.rinelli@kuleuven.be`

NUMERICAL ANALYSIS AND APPLIED MATHEMATICS (NUMA) UNIT, DEPARTMENT OF COMPUTER SCIENCE, KU LEUVEN, LEUVEN, BELGIUM.

Email address: `marc.vanbarel@kuleuven.be`

NUMERICAL ANALYSIS AND APPLIED MATHEMATICS (NUMA) UNIT, DEPARTMENT OF COMPUTER SCIENCE, KU LEUVEN, LEUVEN, BELGIUM.

Email address: `raf.vandebril@kuleuven.be`

NUMERICAL ANALYSIS AND APPLIED MATHEMATICS (NUMA) UNIT, DEPARTMENT OF COMPUTER SCIENCE, KU LEUVEN, LEUVEN, BELGIUM.

Email address: `robbe.vermeiren@kuleuven.be`